

# 1

## Material Properties of Plastics

### 1.1

#### Formation and Structure

The basic structure of plastics (or polymers) is given by macromolecule chains, formulated from monomer units by chemical reactions. Typical reactions for chain assembling are polyaddition (continuous or step wise) and condensation polymerization (polycondensation) [1] (Figure 1.1).

- **Polyaddition as chain reaction:** Process by chemical combination of a large number of monomer molecules, in which the monomers will be combined to a chain either by orientation of the double bond or by ring splitting. No byproducts will be separated and no hydrogen atoms will be moved within the chain during the reaction. The process will be started by energy consumption (by light, heat or radiation) or by use of catalysts.
- **Polyaddition as step reaction:** Process by combination of monomer units without a reaction of double bonds or separation of low molecular compounds. Hydrogen atoms can change position during the process.
- **Polycondensation:** Generation of plastics by build up of polyfunctional compounds. Typical small molecules like water or ammonia can be set free during the reaction. The reaction can occur as a step reaction.

The monomer units are organic carbon-based molecules. Beside carbon and hydrogen atoms as main components elements like oxygen, nitrogen, sulfur, fluorine or chlorine can be contained in the monomer unit. The type of elements, their proportion and placing in the monomer molecule gives the basis for generating different plastics, as shown in Table 1.1.

The coupling between the atoms of a macromolecular chain happens by primary valence bonding [2]. The backbone of the chain is built by carbon atoms linked together by single or double bonding. Given by the electron configuration of carbon atoms, the link between the carbon atoms occurs at a certain angle, for example, for single bonding at an angle of  $109.5^\circ$ . Atoms like hydrogen, which are linked to the carbon atoms, hinder the free rotation of the carbon atoms around the linking axis.

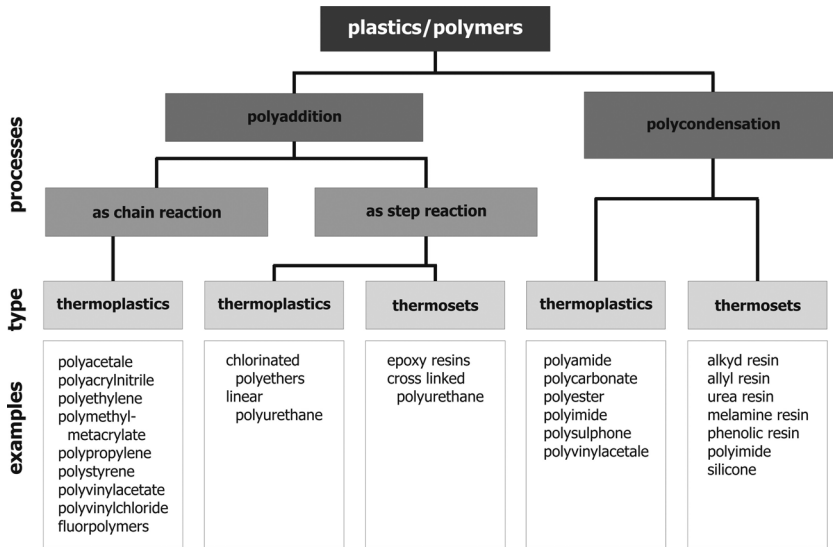


Figure 1.1 Processes for generating plastics and examples [1].

The "cis"-link of carbon atoms has the highest bonding energy while the "trans"-link has the lowest (Figure 1.2) [3].

Depending on the type of bonding partners several chain conformations are possible. Examples of such conformations are zig-zag conformation (e.g., PE or PVC) or helix conformation (e.g., PP, POM or PTFE) (Figure 1.3) [2].

Table 1.1 Examples of some common plastics and their monomers.

	Monomer		Polymer
Ethylene	$\text{CH}_2 = \text{CH}_2$	Polyethylene (PE)	$-\text{[CH}_2 - \text{CH}_2\text{]}_n-$
Propylene	$\begin{array}{c} \text{CH} = \text{CH}_2 \\   \\ \text{CH}_3 \end{array}$	Polypropylene (PP)	$-\text{[CH} - \text{CH}_2\text{]}_n-$ $\quad  $ $\quad \text{CH}_3$
Vinylchloride	$\text{CH}_2 - \text{C} \begin{array}{l} \text{H} \\ \diagup \\ \text{Cl} \end{array}$	Polyvinylchloride (PVC)	$-\text{[CH} - \text{CH}_2\text{]}_n-$ $\quad  $ $\quad \text{Cl}$
Caprolactame		Poly(E-Caprolactame) (PA6)	$-\text{[NH} - (\text{CH}_2)_5 - \overset{\text{O}}{\parallel}{\text{C}}\text{]}_n-$
Tetrafluorethylene $\text{CF}_2 = \text{CF}_2$	Polytetrafluorethylene (PTFE)	$-\text{[CF}_2 - \text{CF}_2\text{]}_n-$	$-\text{[CF}_2 - \text{CF}_2\text{]}_n-$

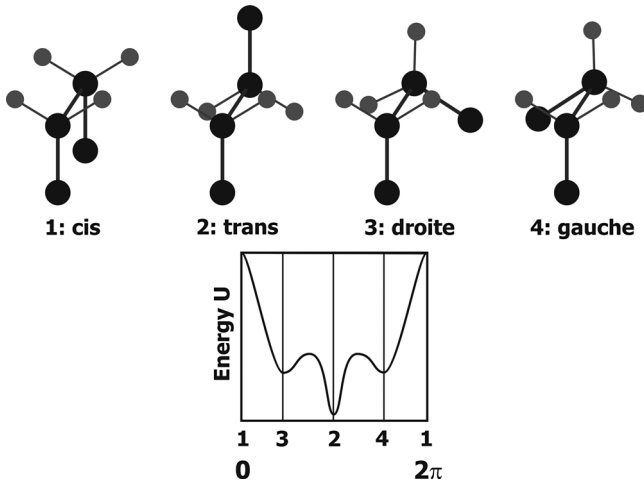


Figure 1.2 Potential energy for rotation of ethylene molecules around the carbon-linking axis [3].

The chain length and by this also the molecular weight of macromolecules have a statistical distribution [4] (Figure 1.4). By influencing the conditions of the polymerization process, the average molecular weight and the width of the distribution function can be controlled within certain limits.

During the polymerization process, depending on the type of polymer, side chains can be built to the main chain in a statistical way [5]. As for the length of the main chain, frequency and length of the side chains depend on the macromolecular structure and the physical/chemical conditions of the polymerization process [6].

An example for the order of size of macromolecules is the length and width of polystyrene molecules with an average molecular weight of  $10^5$ . Corresponding to the molecular weight the macromolecular chain consists of a number of approximately

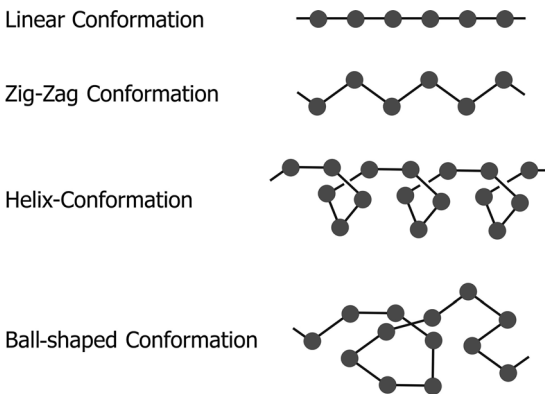
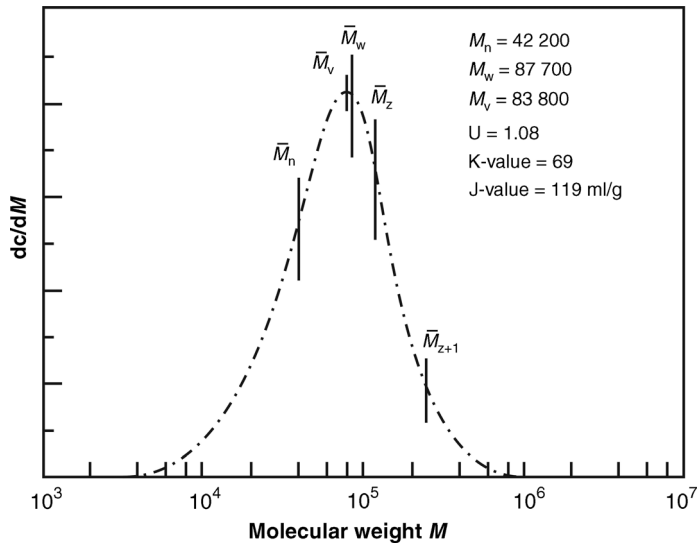


Figure 1.3 Conformation types of macromolecules.



**Figure 1.4** Statistical distribution of macromolecule chain length using polyvinylchloride (PVC) as an example [4].

$2 \times 10^5$  carbon atoms. The average distance between each carbon atom is  $1.26 \times 10^{-10}$  m. Using this distance and the number of atoms in the chain takes to a length of  $25 \times 10^{-6}$  m and  $4\text{--}6 \times 10^{-10}$  m width for a stretched chain.

The statistical forming of the macromolecular structure of plastics results in the fact that physical properties of plastics, like temperatures of phase changes, can only be given as average values. Unlike materials like metals, phase changes of plastics occur in certain temperature ranges. The width of such temperature ranges is dependent on the homogeneity of the materials structure [6].

The physical and chemical structure of the macromolecule is given by the primary valence bonding forces between the atoms (Figure 1.5) [1]. The secondary valence bonding forces, like dispersion bonding, dipole bonding or hydrogen bridge bonds, have a direct influence to the macroscopic properties of the plastic like mechanical, thermal, optical, electrical or chemical properties.

The secondary valence forces are responsible for the orientation of the macromolecules among themselves [6–8]. During processing of plastics the orientation of molecule segments can result in an orientation of segments of the macromolecular chain. Under suitable conditions, like specific placements of atoms in the monomer structure and by this within the macromolecular chain, a partial crystallization of the plastic is possible. The strength of the secondary valences is directly correlated with the formation of the macromolecular chains. The strength increases with increasing crystallization, with higher polarity between the monomer units, decreased mobility of molecule segments and increased strapping of chains with others. Because of the small range and low energy of secondary valences in comparison with the main valences, effects caused by them are strongly temperature dependent.

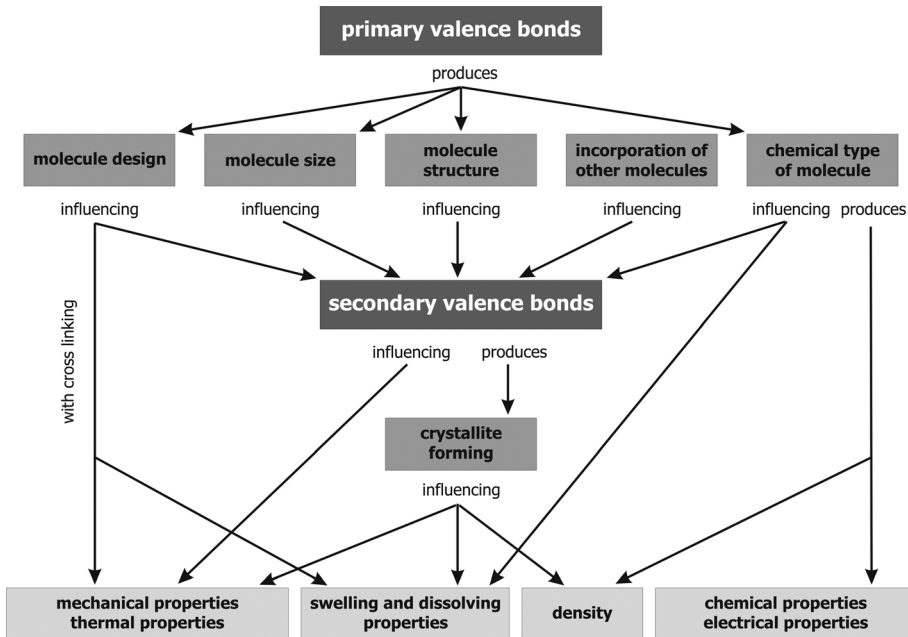


Figure 1.5 Context of molecular and macroscopic material properties [1].

In the case of possible atom bonds between macromolecular chains, a crosslinking of the molecule structure can happen. While secondary valences can be dissolved with increasing temperatures and rebuilt during cooling, atom bonds cannot dissolve reversibly. By dissolving these bonds the plastic will be chemically destroyed.

Taking the chemical structure and the degree of crosslinking between the macromolecules, plastics can be classified as thermoplastics, elastomers and thermosets (Figure 1.6) [1]. Compounds like polymer blends, copolymers and composite materials are composed of several base materials. This composition can be done on a physical basis (e.g., polymer blends or composite materials) or on a chemical basis (copolymers).

## 1.2

### Types of Plastics

Caused by the macromolecular structure and the temperature-dependent physical properties plastic materials are distinguished into different classes. Figure 1.7 gives an overview of the classification of plastics with some typical examples.

Thermoplastics are in the application range of hard or tough elasticity and can be melted by energy input (mechanical, thermal or radiation energy). Elastomers are of soft elasticity and usually cannot be melted. Thermosets are in the application range of hard elasticity and also cannot be melted.

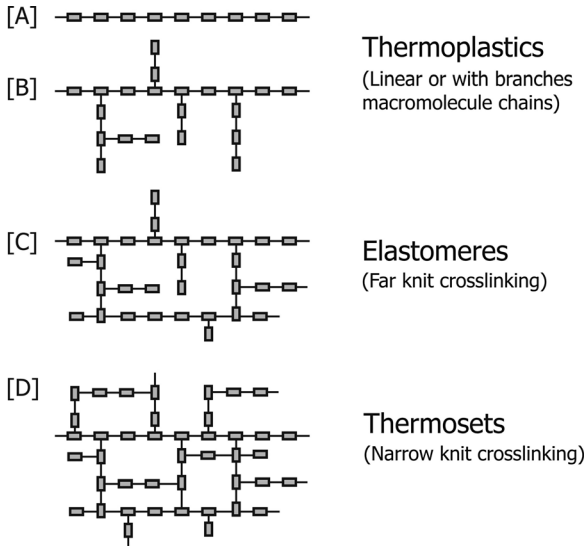


**Figure 1.6** Principle structure of linear (A), with side chains (B) and crosslinked macromolecules (C + D). Chain structure (A) and (B) are thermoplastic types, structures with low crosslinking (C) elastomers and with strong crosslinking thermosets (D).

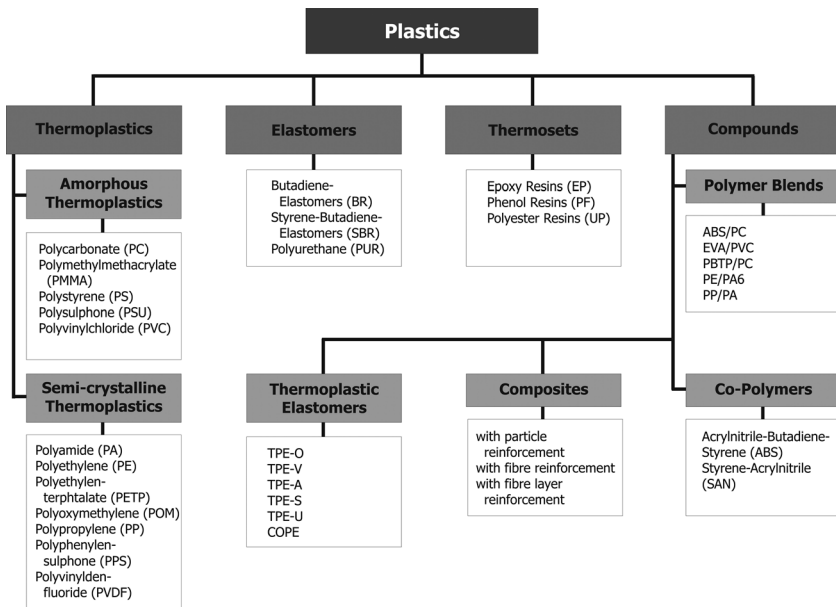


**Figure 1.7** Classification of plastics.

Plastics as polymer mixtures are composed of two or more polymers with homogeneous or heterogeneous structure. Homogeneous structures are for example copolymers or thermoplastic elastomers, built by chemical composition of two or more different monomer units in macromolecules. When using thermoplastic monomers such plastic material can be melted by thermal processes. Heterogeneous structures are for example polymer blends or thermoplastic elastomers, built by physical composition of separate phases from different polymers. Polymer blends with thermoplastic components also can be melted by thermal processes.

Plastic composites consist of a polymeric matrix with integrated particles or fibers. When using thermoplastics as matrix, such composites can be melted. If thermosets are used as matrix the composite cannot be melted.

Characteristic of the different classes of plastics are the phase transitions that occur in contrast to metallic materials in temperature intervals. Data given in tables (e.g., [9]), are usually mean values of such temperature intervals.

Phase-transition temperatures are dependent on the molecular structure of the plastic. Limited mobility of the molecule chains, for example, by loop forming, long side chains or high molecular weight cause an increased phase-transition temperature [6]. A large variance of the molecule chain length or number and length of side chains also have an effect on the spreading of the phase-transition ranges.

### 1.2.1

#### **Thermoplastic Resins**

Thermoplastic resins consist of macromolecular chains with no crosslinks between the chains. The macromolecular chains themselves can have statistical oriented side chains or can build statistical distributed crystalline phases. The chemistry and structure of thermoplastic resins have an influence on the chemical resistance and resistance against environmental effects like UV radiation. Naturally, thermoplastic resins can vary from optical transparency to opaque, depending on the type and structure of the material. In opaque material, the light is internally scattered by the molecular structure and direct transmission of light is very poor with increasing material thickness.

Thermoplastic resins can be reversibly melted by heating and resolidified by cooling without significant changing of mechanical and optical properties. Thus, typical industrial processes for part manufacturing are extrusion of films, sheets and profiles or molding of components.

The viscosity of the melt is dependent on the inner structure, like average molecular weight and spreading of the molecular weight around the average value. According to DIN EN ISO 1133:2005–2009 [10], the melt-flow index (MFI) is a measure for the melt viscosity. The MFI gives the amount of material that will be extruded in 10 min through a standardized nozzle diameter by using a determined force.

Low MFI values signify high viscosity with glutinous flow behavior of the melt (materials for extrusion). Increasing MFI values result in decreasing viscosity and lighter melt flow behavior (materials for molding). It has to be noted that MFI values

**Table 1.2** Examples for amorphous thermoplastic resins with typical material properties according to [1].

Resin	Temperature of use [°C]	Specific weight [g/cm <sup>3</sup> ]	Tensile strength [N/mm <sup>2</sup> ]
PC	−40–120	1.2	65–70
PMMA	−40–90	1.18	70–76
PS	−20–70	1.05	40–65
PSU	−100–160	1.25	70–80
PVC	−15–60	1.38–1.24	40–60

are only a rough estimation for the melt flow behavior because the structure viscosity of thermoplastics strongly depend on the loading [11].

The macromolecular structure of thermoplastics is given by the chemical structure of the monomer units, the order of the monomer units in the molecule chain and the existing side chains. A pure statistical distribution of the macromolecules results in an amorphous material structure, but also semicrystalline structures can occur depending on the material. Therefore, thermoplastic resins are differentiated into amorphous and semicrystalline types [1, 6].

#### 1.2.1.1 Amorphous Thermoplastics

Amorphous thermoplastic resins consist of statistical oriented macromolecules without any near order. Such resins are in general optically transparent and mostly brittle. Typical amorphous thermoplastic resins are polycarbonate (PC), polymethylmethacrylate (PMMA), polystyrene (PS) or polyvinylchloride (PVC).

Table 1.2 shows examples of amorphous thermoplastic resins with typical material properties.

Temperature state for application of amorphous thermoplastic resins is the so called glass condition below the glass temperature  $T_g$ . The molecular structure is frozen in a definite shape and the mechanical properties are barely flexible and brittle (Figure 1.8).

On exceeding the glass temperature, the mechanical strength will decrease by increased molecular mobility and the resin will become soft elastic. On reaching the flow temperature  $T_f$  the resin will come into the molten phase. Within the molten phase the decomposition of the molecular structure begins by reaching the decomposition temperature  $T_d$ .

#### 1.2.1.2 Semicrystalline Thermoplastics

Semicrystalline thermoplastic resins consist of statistical oriented macromolecule chains as amorphous phase with embedded crystalline phases, built by near-order forces. Such resins are usually opaque and tough elastic. Typical semicrystalline thermoplastic resins are polyamide (PA), polypropylene (PP) or B (POM) (Table 1.3).

The crystallization grade of semicrystalline thermoplastic depends on the regularity of the chain structure, the molecular weight and the mobility of the molecule chains, which can be hindered by loop formation [6]. Due to the statistical chain



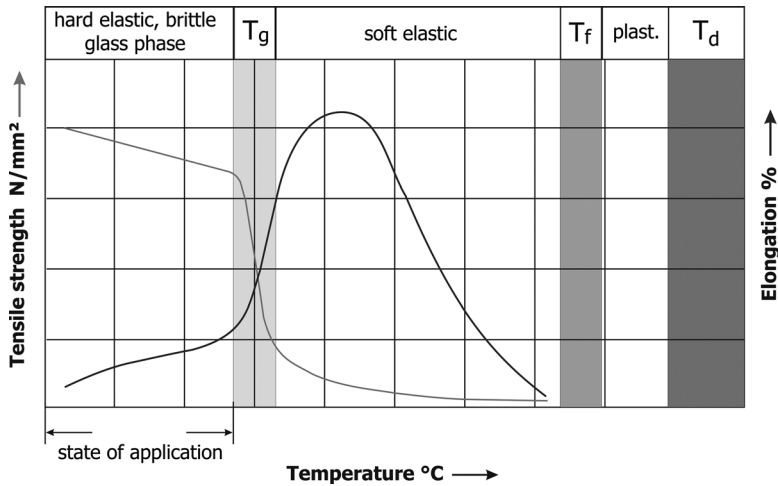


**Figure 1.8** Temperature behavior of amorphous thermoplastic resins (schematically) [1].

structure of plastics complete crystallization is not feasible on a technical scale. Maximum technical crystallization grades are of the order of approximately 80% (see Table 1.3).

The process of crystallization can be controlled by the processing conditions. Quick cooling of the melt hinders crystallization. Slowly cooling or tempering at the crystallization temperature will generate an increased crystallization grade. Semicrystalline thermoplastics with low crystallization grade and small crystallite phases will be more optically transparent than materials of high crystallization grade and large crystallite phases.

Below the glass temperature  $T_g$  the amorphous phase of semicrystalline thermoplastics is frozen and the material is brittle (Figure 1.9). Above the glass temperature, usually the state of application [1], the amorphous phase thaws and the macromolecules of the amorphous phase gain more mobility. The crystalline phase still exists and the mechanical behavior of the material is tough elastic to hard. Above the

**Table 1.3** Examples for semicrystalline thermoplastic resins with typical material properties according to [1].

Resin	Temperature of use [°C]	Crystallization grade [%]	Specific weight [g/cm <sup>3</sup> ]	Tensile strength [N/mm <sup>2</sup> ]
PA 6	-40–100	20–45	1.12–1.15	38–70
HDPE	-50–90	65–80	0.95–0.97	19–39
PETP	-40–110	0–40	1.33–1.38	37–80
PP	-5–100	55–70	0.90–0.91	21–37
PPS	<230	30–60	1.35	65–85
PVDF	-30–150	-52	1.77	30–50

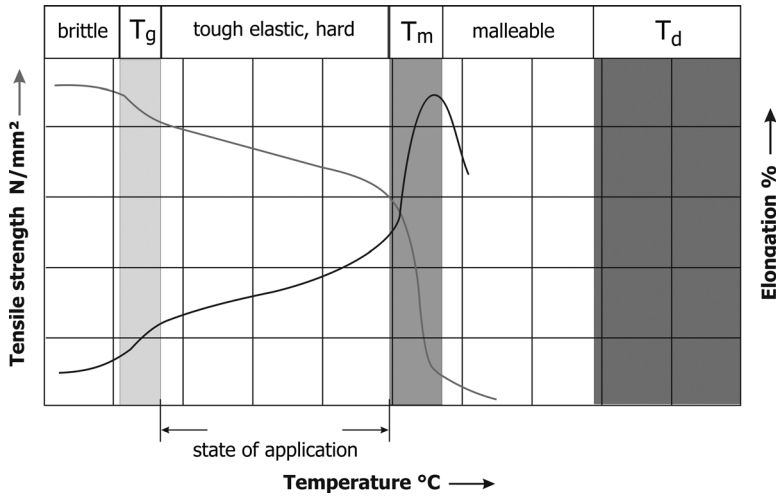


Figure 1.9 Temperature behavior of semicrystalline thermoplastic resins (schematically) [1].

crystal melt temperature  $T_m$  the crystalline phase also starts to melt and the material becomes malleable. As for amorphous thermoplastics, the flow ability of semicrystalline thermoplastics in the molten phase is characterized by the melt-flow index MFI.

The melt temperature of semicrystalline thermoplastics depends among other things on the size of the crystallites and the ratio between the amorphous and crystalline phases. Larger size and a higher proportion of crystallites will increase the melt temperature (Figure 1.10) [12]. As with amorphous thermoplastics, degradation of semicrystalline thermoplastics will start in the molten phase by exceeding the decomposition temperature  $T_d$ .

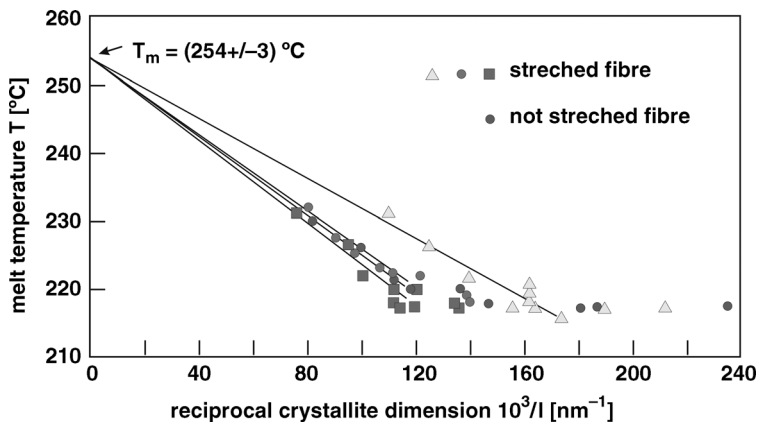


Figure 1.10 Influence of the crystallite size to the melt temperature for PA6 fiber material [12].

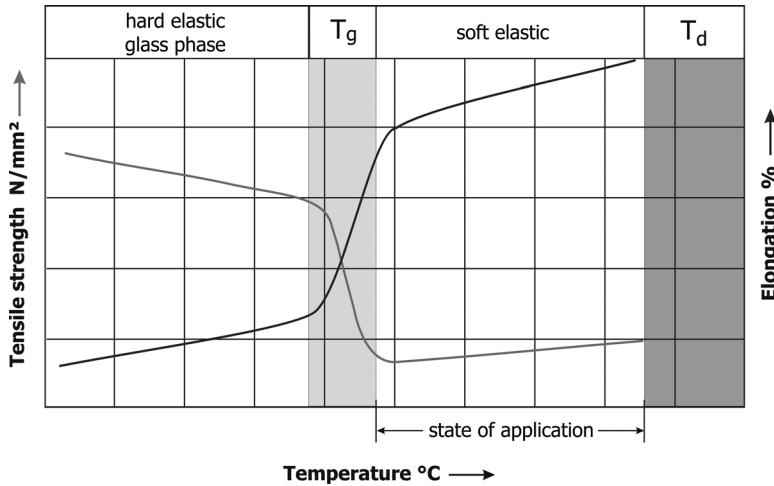


Figure 1.11 Temperature behavior of mechanical properties of elastomers (schematically) [1].

### 1.2.2

#### Elastomers

Elastomers are plastics with wide netlike crosslinking between the molecules. Usually, they cannot be melted without degradation of the molecule structure. Above the glass temperature  $T_g$ , as the state of application (Figure 1.11), elastomers are soft elastic. Below  $T_g$  they are hard elastic to brittle. The value of the glass temperature increases with increasing number of crosslinks. Examples of elastomers are butadiene resin (BR), styrene butadiene resin (SBR) or polyurethane resin (PUR) [13].

Raising temperature affects an increase of elasticity, caused by reducing the stiffening effects of the crosslinks and increasing the mobility of the molecule chains. On exceeding the decomposition temperature  $T_d$ , the atom bonding within and between the molecule chains will be broken and the material will be chemical decomposed.

### 1.2.3

#### Thermosets

Thermosets are plastic resins with narrow crosslinked molecule chains [1]. Examples of thermosets are epoxy resin (EP), phenolic resin (PF) or polyester resin (UP).

In the state of application (Figure 1.12) thermosets are hard and brittle. Because of the strong resistance of molecular movement caused by the crosslinking, mechanical strength and elasticity are not temperature dependent, as with thermoplastics or elastomers.

Thermosets cannot be melted and joining by thermal processes like ultrasonic welding or laser welding is not possible. On exceeding the decomposition temperature  $T_d$ , the material will be chemical decomposed.

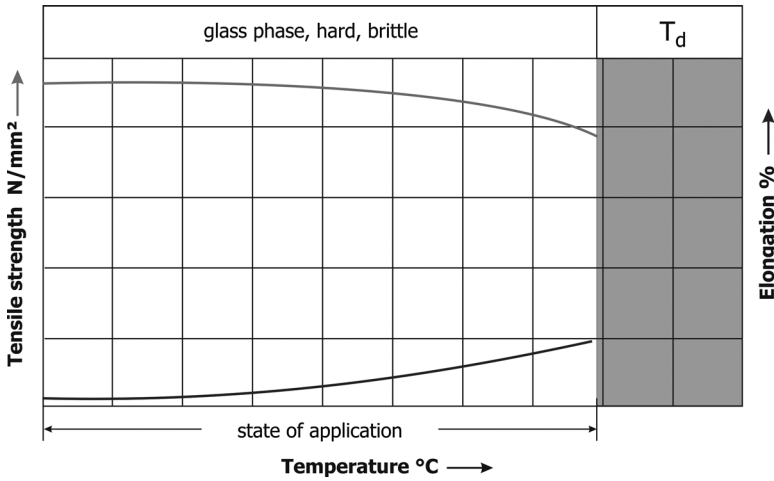


Figure 1.12 Temperature behavior of mechanical properties of thermosets (schematically) [1].

#### 1.2.4

#### Polymer Compounds

The term polymer compound summarizes materials like polymer blends, copolymers and thermoplastic elastomers (TPEs). Polymer compounds are physical or chemical composed from different polymers to achieve special material properties like elasticity or fatigue strength.

##### 1.2.4.1 Polymer Blends

Polymer blends are combinations of different polymers [14], usually mixed in the molten state. After solidification the different polymeric proportions are combined by physical but not chemical reaction (Figure 1.13).

The extent to which a mixture can be achieved depends on the miscibility of the polymers among each other. Chemical, thermal or mechanical properties of polymer

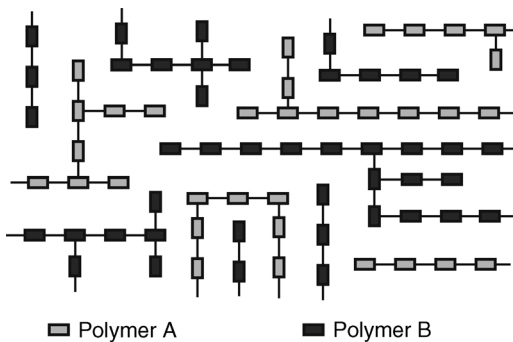


Figure 1.13 Schematic molecule structure of polymer blends.

**Table 1.4** Examples of thermoplastic polymer blends. Condition of application, specific weight and typical mechanical strength [15].

Resin	Temperature of use [°C]	Specific weight [g/cm <sup>3</sup> ]	Tensile strength [N/mm <sup>2</sup> ]
PC/ABS	<90	1.10–1.16	45–55
PC/ASA	<105	1.15	53–63
PPE/SB	<100	1.06	52–64

blends are defined by the type of different polymers used and their proportions within the polymer blend.

Polymer blends, designed from thermoplastic materials, can be joined together by thermal processes like ultrasonic or laser welding. Examples of thermoplastic polymer blends are PC/ABS, PC/ASA or PPE/SB (see Table 1.4).

#### 1.2.4.2 Copolymers

Copolymers are built by chemical composition at least from two different monomer units. Processes to built up copolymers are block polymerization, group transfer polymerization or graft copolymerization [1, 6, 16]. Examples of copolymers are ABS or SAN (see Table 1.5).

Beside grade of polymerization, chain-length distribution, type of end groups and chain side branches, composition and distribution of monomer units inside the molecule chain have to be known to achieve specific chemical, thermal, optical or mechanical properties of the copolymer. Especially influential on the properties is the regularity of the chain composition, which means a statistical or more regular distribution of the different monomers within the molecule chain (Figure 1.14) [11].

#### 1.2.4.3 Thermoplastic Elastomers

Thermoplastic elastomers (TPEs) are elastic, flexible polymers with similar qualities as elastomers or rubber but of a thermoplastic nature [17, 18]. TPEs close the gap between stiff thermoplastics and vulcanized elastomers. Due to the thermoplastic nature, TPEs can be processed to parts by extrusion and molding and can also be joined together or to other thermoplastic material by adhesive bonding, solvent bonding and welding processes or by coextrusion and multicomponent injection molding.

**Table 1.5** Examples of thermoplastic copolymers. Conditions of application, specific weight and typical mechanical strength [1].

Resin	Temperature of use [°C]	Specific weight [g/cm <sup>3</sup> ]	Tensile strength [N/mm <sup>2</sup> ]
ABS	–30–95	1.04	38–58
COC	–50–130	1.02	46–63
SAN	–20–80	1.08	70–79

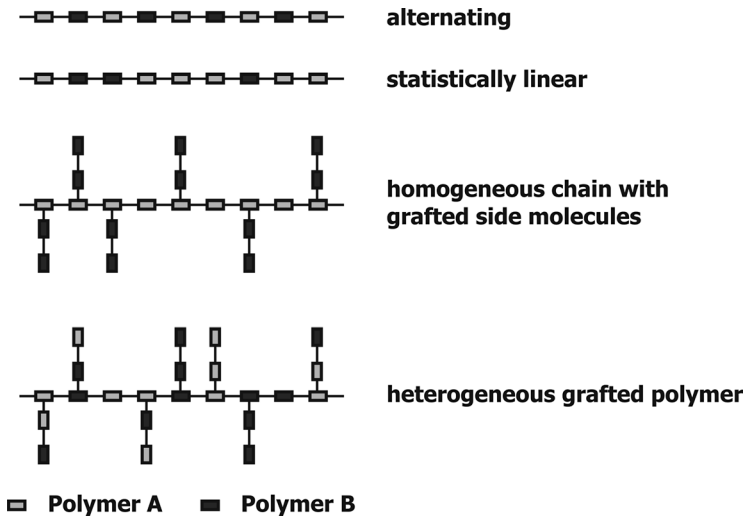


Figure 1.14 Schematic build up of copolymers.

In principal, the material group of TPEs consists of two different base structures as a physical or chemical mixture, polymeric blends and block copolymers. Depending on the molecular structure given by the thermoplastic component, both of them could be amorphous or semicrystalline.

*TPE blends* consist of a thermoplastic matrix, for example, PP or PE, and softer particles, for example, EPDM, which are well dispersed in the matrix (see Figure 1.15). Two types of TPE blends are available:

- Thermoplastic vulcanization elastomers (TPE-V): are TPE blends with a chemically crosslinked elastomer proportion produced by dynamic vulcanization that is a process of intimate melt mixing of a thermoplastic polymer like PP and a suitable reactive elastomer like EPDM.
- Thermoplastic polyolefin elastomers (TPE-O): two-component elastomer systems consisting of elastomers like EPR and EPDM finely dispersed in a thermoplastic polyolefin (e.g., PP).

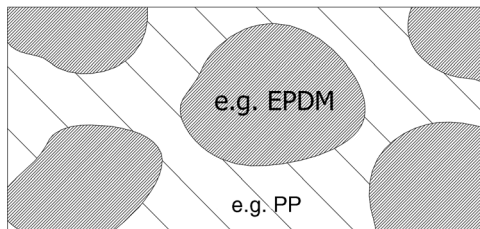
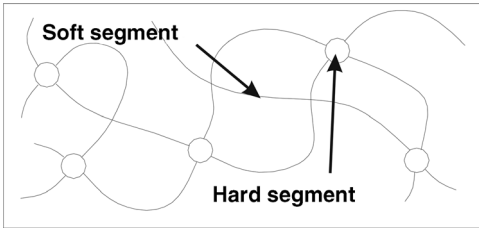


Figure 1.15 Schematic structure of TPE blends [18].



**Figure 1.16** Schematic structure of TPE block copolymers [18].

In *block copolymers*, the hard and soft segments are linked within the macromolecules (Figure 1.16). Materials used as hard segments are for example, styrene and for soft segments butylenes. Common block copolymers are:

- Styrene block copolymers (SBC, TPE-S): consist of block segments of styrene monomer units and elastomer monomer units. Their most common structure are linear A–B–A block type: styrene-butadiene-styrene (SBS), styrene-isoprene-styrene (SIS), styrene-ethylene/butylenes-styrene (SEBS) or styrene-ethylene/propylene-styrene (SEPS) type.
- Thermoplastic polyurethane elastomers (TPE-U): were first commercialized in the 1950s and are one of the oldest TPE types in existence.
- Copolyester elastomers (COPE): are a family of engineering thermoplastic elastomers based on copolyester chemistry. They have both hard and soft parts. The hard segment is a semicrystalline polybutylene terephthalate (PBT), while the soft segment is made of amorphous glycol.
- Copolyamides (COPA, TPE-A): also called polyether block amides (PEBA), are extremely versatile, high-performance engineering thermoplastic elastomers that combine the properties of nylon and elastomers. The polymer structure consists of a regular linear chain of rigid polyamide segments, usually based on polyamide PA 6 or high-performance PA12 infiltrated with flexible polyether segments.

Depending on the type of TPE, a wide variation from very soft to more rigid materials is given. The hardness values can vary in a wide range of shore A values. Table 1.6 gives an overview about typical thermal and mechanical properties of TPEs.

**Table 1.6** Examples of thermoplastic elastomers. Condition of application, specific weight and typical hardness values [18].

Resin	Temperature of use [°C]	Specific weight [g/cm <sup>3</sup> ]	Shore A hardness
TPE-A	–40–170	1.01	70–90
TPE-E	–65–150	>1	70–80
TPE-U	–50–135	>1	70–90
TPE-O	–60–110	0.89–1.00	40–90
TPE-V	–60–110	0.89–1.00	40–90
TPE-S	–50–100	0.89–1.30	10–90

**Table 1.7** Examples for thermoplastic composites with glass fibers. Condition of application, proportion of glass fibers, specific weight and typical mechanical strength [15].

Resin	Temperature of use [°C]	Proportion of glass fibers [%]	Specific weight [g/cm <sup>3</sup> ]	Tensile strength [N/mm <sup>2</sup> ]
PA6/GF30	<200	30	1.36	65–170
PC/GF30	<140	30	1.44	70–110
PP/GF30	<110	30	1.11–1.14	60–100
PPS/GF60	<240	60	1.90	170
PC/ABS/GF20	<95	20	1.25	75

Because of low melting temperatures TPEs can easily be processed by molding or extrusion within a temperature range of 190–240 °C (depending on the TPE type). But to achieve a good homogenization during the processing high shear forces have to be used.

Uncolored TPEs can vary from optical transparency to opaque, depending on type and structure of the material. In opaque material, the light is internally scattered by the molecular structure and direct transmission of light is very poor with increasing material thickness.

Most of the TPEs show good weather and chemical resistance. Natural TPEs are usually colorless transparent or opaque and can be easily colored.

### 1.2.5

#### Polymer Composites

Polymer composites are composed of a polymer matrix material (thermoplastic or thermosets) with organic or inorganic fillers (Figure 1.17) [1] like mineral pigments, short fibers, long fibers, continuous fibers, paper or fabrics to enhance the mechanical properties for special applications.

Particles like mineral powder, wood flour or carbon black are used to increase the stiffness of the matrix material. The fatigue strength of the matrix material usually will be not increased, but is sometimes decreased. Short fibers, long fibers and continuous fibers from glass, carbon or aramid cause an increase of the fatigue strength (Figure 1.18), although the effect depends on the orientation of the fibers [19].

Continuous fibers from glass, carbon or aramid will influence the mechanical properties of the polymer compound by the adjustable orientation of the fibers. Besides increasing fatigue strength and stiffness the temperature-dependent expansion of the compound can also be decreased [20].

Polymer compounds with thermoplastic matrix usually can be melted by thermal processes like welding, but not polymer compounds with thermoset matrix.



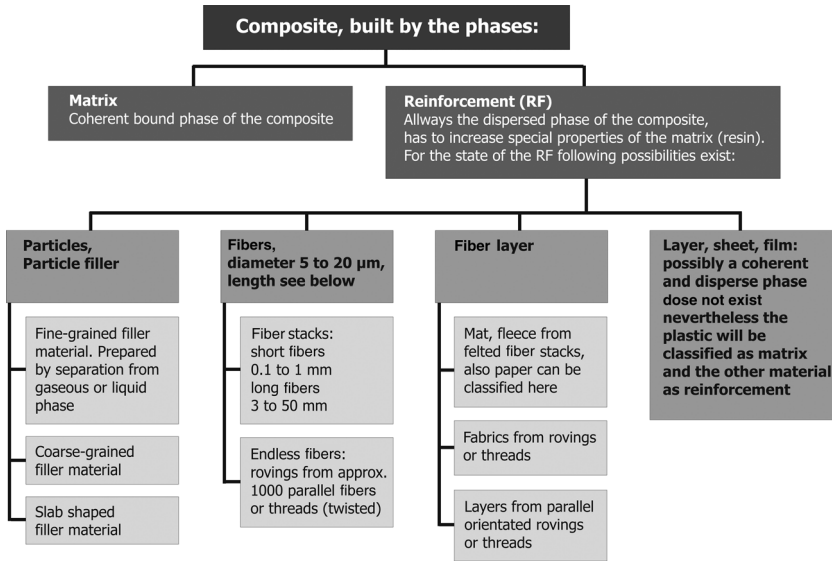


Figure 1.17 Classification of polymer composites [1].

### 1.3 Thermal Properties

Successful processing of thermoplastic resins by laser radiation needs a basic knowledge of the temperature dependence of the thermal material properties. The temperature ranges of the different phase transitions (e.g., glass transition and softening temperatures of amorphous thermoplastics, melt temperatures of crystalline phases of semicrystalline thermoplastics) but also material properties linked

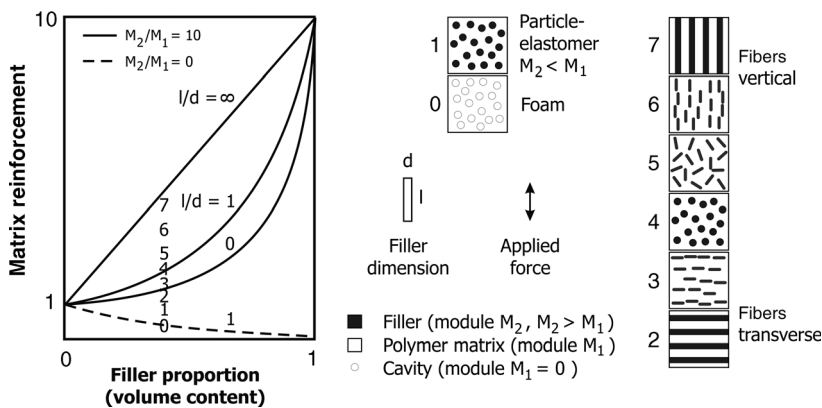


Figure 1.18 Dependence of the reinforcement on the type and structure of the filler material [11].

with heat conduction (e.g., heat capacity, heat conduction or specific volume) influence of laser power and processing speed of a laser application.

Thermal properties of thermoplastics strongly depend on the molecular structure. Orientation and length of macromolecular chains, number and distribution of side chains, crystalline structure or level of molecular links influence such thermal properties.

Typical phase transitions of thermoplastic resins are glass transition, melting of crystallites and thermal degradation of macromolecular chains. Physical properties like specific volume, heat capacity, heat conduction or thermal conduction, which characterize the material behavior regarding thermal energy absorption and transport, partly show a distinctive dependence of the material temperature and vary particularly in the ranges of phase transitions.

### 1.3.1

#### Phase Transitions

Depending on the physical and chemical structure of thermoplastic resins, the following phase transitions will occur on increasing material temperature [1, 6]:

##### 1.3.1.1 Glass Transition ( $T_g$ )

Below the glass temperature ( $T_g$ ) the mobility of the molecules (Brown's macromobility) is strongly curbed by intermolecular interaction. There are no position-change processes and only restricted thermal induced movements of chain segments or side chains. At the glass temperature Brown's micromobility of chain segments and side chains starts to occur and the plastic becomes softer but is still mechanical stable. Before reaching the glass temperature second-order relaxation processes are possible, single-molecule segments obtain a restricted mobility.

##### 1.3.1.2 Flow Temperature ( $T_f$ )

On increasing temperature the hindering influence of intermolecular interaction decreases. On reaching the flow temperature ( $T_f$ ) complete macromolecular chains can slip against each other (Brown's macromobility). The amorphous structures of the plastic become softer and start to melt. No chemical degradation of the macromolecules of the plastic will occur in this state.

##### 1.3.1.3 Crystallite Melting Temperature ( $T_m$ )

By reaching the crystallite melting temperature ( $T_m$ ) of semicrystallite thermoplastics the near forces, responsible for crystallite forming, will vanish and the crystallites start to melt. Because the temperature range of crystallite melting exceeds the flow temperature of the amorphous state, the entire thermoplastic will be plasticized. As long as no thermal degradation will occur in the molten phase, the resin can reversibly get back into the solidified state by cooling. Depending on the cooling conditions (speed and duration of cooling) crystallite phases will again be generated. The size and distribution of these crystallites can be differing from the original status.

**Table 1.8** Examples for phase-transition temperatures for thermoplastic resins [1, 6].

Resin	Glass temp. $T_g$ (°C)	Flow temp. $T_f$ (°C)	Crystallite melt temp. $T_m$ (°C)	Decomposition temp. $T_d$ (°C)
Amorphous Thermoplastics				
PC	145	240		about 327
PMMA	104	180		226–256
PS	97	160		318–348
PVC	80	175		about 250
Semicrystalline Thermoplastics				
HDPE	–95		130–146	360–390
PA 6	40		220	about 327
PEEK	120		340	
PP	–18		160–208	336–366
PTFE	–20		327	424–513

#### 1.3.1.4 Thermal Decomposition ( $T_d$ )

Exceeding the decomposition temperature ( $T_d$ ) in the molten phase of thermoplastics and thermoplastic elastomers, the macromolecules start to decompose caused by intensive thermal oscillations. Separation of monomer units (e.g., PMMA) [6], oxidation or chemical conversion into reaction products like HCl during decomposition of PVC are possible reactions [4]. The resin will be irreversibly chemically modified.

The decomposition products will be separated as gaseous phase or will remain as components in the residual material. The start of decomposition, which means the value of the decomposition temperature, is greatly dependent on the intensity and duration of the thermal input. The decomposition temperature is lower by long duration and low intensity than by short duration and high intensity of the thermal input.

For laser welding of thermoplastic resins and thermoplastic elastomers phase transitions in the thermal range from room temperature up to the start of degradation are of interest. Table 1.8 summarizes phase-transition temperatures of typical thermoplastic resins. The indicated temperatures refer to average values or temperature ranges of phase transitions.

Plasticization of amorphous thermoplastics starts with exceeding the flow temperature ( $T_f$ ) and for semicrystalline thermoplastics with exceeding the crystallite melting temperature ( $T_m$ ). Figure 1.19 shows for a number of thermoplastics a compilation of the temperature ranges of the molten phase and the start of decomposition (from [1]). The decomposition temperatures in Table 1.8 or Figure 1.19 are dependent on the reference values of thermal degradation under vacuum [21] or estimated values (from [1]) and can possibly differ somewhat under atmospheric influence.

Increasing the temperature of a solid material will be done by energy input for example, using friction energy, ultrasonic energy or absorption of radiation. In the

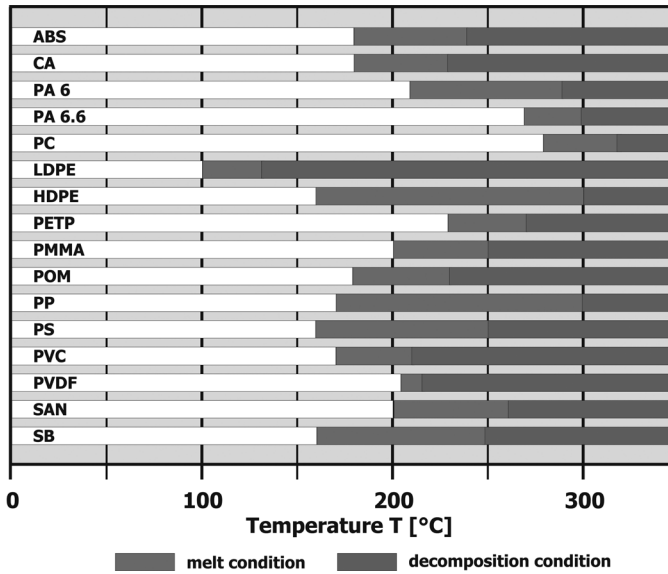


**Figure 1.19** Melt-temperature ranges and decomposition in the molten state of some thermoplastic resins [1].

range of phase transitions an additional energy input is necessary to start the phase transition. For amorphous thermoplastics phase transition will occur at the flow temperature and for semicrystalline thermoplastics at the crystallite melting temperature. To start a phase transition an additional energy input as melting energy (or melting enthalpy) is necessary. The height of the melting energy for semicrystalline thermoplastics is dependent on the grade of crystallinity of the material.

Table 1.9 gives examples of the melting energy relative to the mass proportion of the crystalline phase of semicrystalline thermoplastics.

### 1.3.2

#### Specific Volume

The volume of thermoplastics expands with increasing temperature. Caused by more intense thermal oscillation of atoms and molecule elements the balance positions of

**Table 1.9** Melt energy for some typical semicrystalline thermoplastics [1].

Resin	Melting Energy $\Delta$ [J/g]
HDPE	310
PA 6	213
PETP	145
POM	333
PP	238

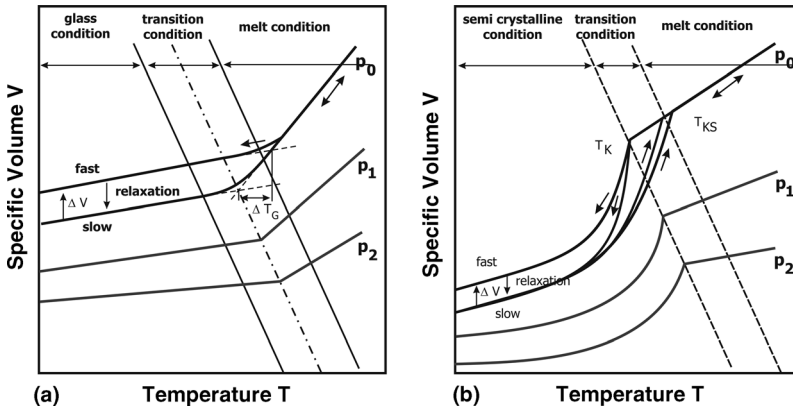


**Figure 1.20** Schematic behavior of specific volume in dependence from the temperature for amorphous (a) and semicrystalline thermoplastics (b) [23].

the oscillation segments are moving apart [22]. As for example, heat capacity or heat conductivity, the type of bonding and caused by this the material structure is an important influence on the quantity of the volume change. For the temperature dependence of the specific volume a distinction is given between amorphous and semicrystalline plastics (Figures 1.20a and b) [23].

Within the glass state of amorphous thermoplastics the specific volume shows a linear increase with increasing temperature (see Figure 1.20a) [23], described by Equation 1.1:

$$V(T) = V_0(1 + \beta \cdot \Delta T) \quad (1.1)$$

$V_0$ : volume at start of heating  
 $\beta$ : cubic expansion coefficient  
 $\Delta T$ : increase of temperature.

On exceeding the glass-transition temperature the linear increase rapidly rises, depending on the distribution of the molecular weight. This means with increasing temperature the increase of the specific volume will be intensified, caused by decreasing strength of molecular bonds in the molten state. In Figure 1.21a a graphic portrayal of the temperature-dependent course of the specific volume for some amorphous thermoplastics is given.

Below the glass temperature the volume change of semicrystalline thermoplastics rises almost linearly with increasing temperature. On exceeding the crystallite melting temperature a difference to the linear behavior occurs. The volume change on increasing temperature will be almost linear again if the plastic is completely plasticized. Figure 1.21b shows the temperature-dependent course of the specific volume from some semicrystalline thermoplastics.

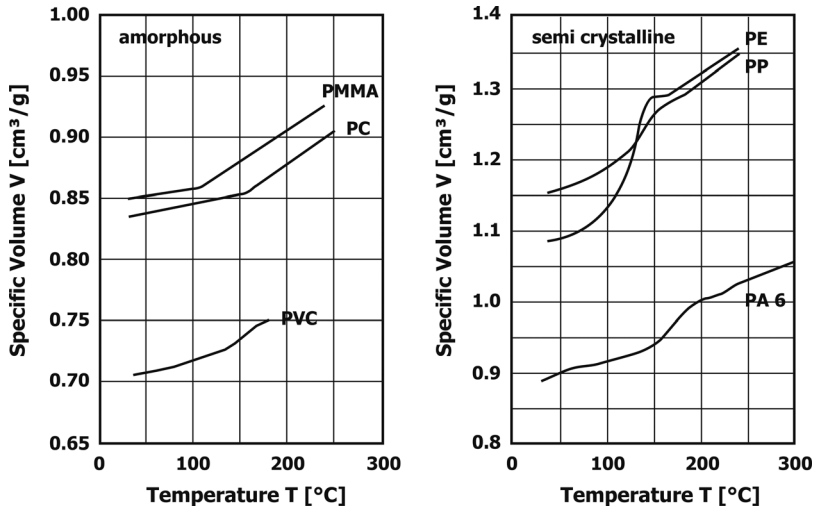


**Figure 1.21** Specific volume of amorphous (left) and semicrystalline thermoplastics (right) in correlation with the temperature [23].

Depending on the cooling rate out of the molten state a different crystallization of the thermoplastic material can occur [24]. The faster the cooling the smaller will be the crystalline phases in dimension and they will be less numerous. The specific volume of a fast-cooled semicrystalline thermoplastic with low crystallization will be higher than of a slowly cooled material with high crystallization.

### 1.3.3

#### Heat Capacity

The heat capacity of a solid material is fixed by the ability of individual components (atoms, molecule segments or molecule chains) to carry out oscillations around their center positions [25]. Among other influences the strength of such oscillations is dependent on the bonding forces and the weight of atoms or molecule segments (molar weight). The oscillations are an addition of individual grid oscillations of atoms bound in a macromolecule, of group oscillations of molecular segments (elongation or tilt oscillations) and rotation oscillations of molecular segments.

Due to the covalent bonding of segments within the molecule chain and the coupling of molecule chains among themselves (e.g., second-order valence bonding, hydrogen bridge bonding or dipole bonding) the individual oscillations are not independent of each other. The individual oscillations will be composed of collective oscillations that will be spread as waves in all directions of the material. The frequency spectrum of the grid oscillations reaches from translation of the whole grid (frequency zero) up to maximum frequencies of  $10^{13}$  to  $10^{14}$  Hz caused by intermolecular bonding forces and the weight of the molecules.

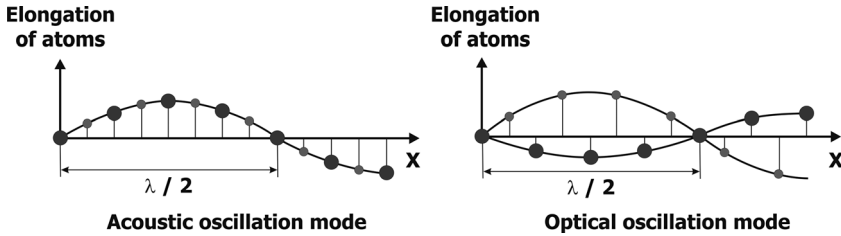


**Figure 1.22** Principle portrayal of acoustic (left) and optical (right) oscillation modes of the grid segments. from [22].

Between adjoining grid segments in the molecule chain strong covalent bonding forces are prevalent while between different molecular chains considerably weaker bonding forces like van der Waals or dipole bonding exists [6]. The frequency spectrum of oscillations corresponds up to approximately  $10^{12}$  Hz to a three-dimensional solid body. For higher frequencies the spectrum will change to the oscillation spectrum of isolated chain molecules [25].

The oscillation spectrum can be divided up into an acoustic and an optical mode. In the acoustic mode the grid segments are elongated in the same direction. In the optical mode the adjoining grid segments oscillate in contrary elongations (Figure 1.22) [22].

The optical mode of grid oscillations can be stimulated by absorption of electromagnetic radiation. By oscillation coupling between optical and acoustic modes an energy transfer occurs from optical to acoustical modes. A schematic drawing of the frequency spectrum for a linear molecule chain with two segments of alternating weights  $M_A$  and  $M_B$  are shown in Figure 1.23 for different mass proportions.

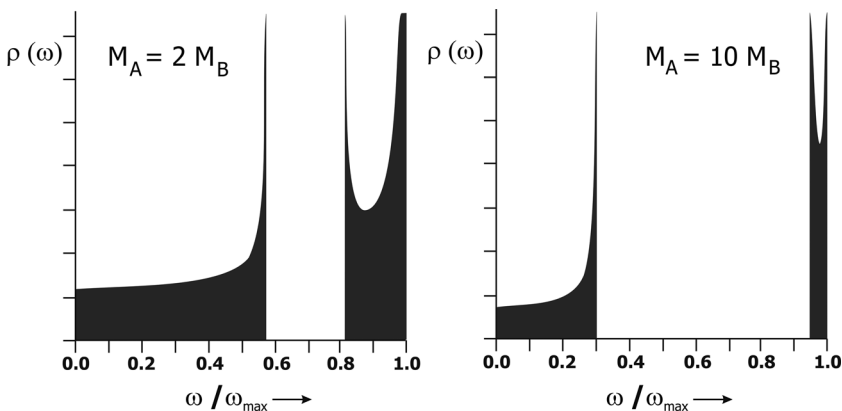


**Figure 1.23** Frequency spectrum of an oscillating linear molecule chain with alternating segments of weights  $M_A$  and  $M_B$  [21].

The heat capacity at constant volume  $c_v$  is given by integration (Equation 1.2) over the entire oscillation spectrum [21]:

$$c_v = k \cdot \int \left( \frac{\hbar\omega}{kT} \right)^2 \cdot \frac{\exp(\hbar\omega/kT)}{(\exp(\hbar\omega/kT)-1)^2} \varrho(\omega) d\omega \quad (1.2)$$

$\hbar$ : Planck constant

$\omega$ : oscillation frequency

$k$ : Boltzmann constant

$T$ : temperature

$\varrho(\omega)$ : density distribution of oscillation spectrum.

The density distribution  $\varrho(\omega)$  of the oscillation spectrum is standardized by following equation:

$$\int \varrho(\omega) d\omega = 3N \quad (1.3)$$

$N$ : numbers of oscillation centers.

In general, an exact evaluation of Equation 1.2 is not possible because of an unknown density distribution of the oscillation spectrum [21]. The starting point for an approach is given by the models from Einstein and Debye [25]. The acoustic mode of the oscillation will be described by Debye's approach and the optical mode by Einstein's approach [26, 27].

Consideration of the heat capacity at constant volume  $c_v$  enables a theoretical determination of molecule chain oscillations induced by acoustic or optical waves, related with the heat capacity. In contrast to the heat capacity at constant pressure  $c_p$ , the heat capacity  $c_v$  cannot be measured, however. Therefore, for computation of temperature distributions in the material by numerical or analytical computer simulation the heat capacity  $c_p$  is of practical importance.

Caused by interaction processes within and between molecule chains and the temperature dependence of such processes, the heat capacity  $c_p$  of thermoplastics is also dependent on the temperature. In the state of melting the heat capacity increases caused by the melt heat (also called melt enthalpy) as an additional energy need for generating the phase shift.

Especially for semicrystalline thermoplastics the heat capacity  $c_p$  has a significant discontinuousness in the state of melting. After all crystalline phases are melted the value of the heat capacity will decrease back to the value before reaching the molten state. By melting of the crystallites a lot of oscillation modes will be activated that were hindered before by the first-order forces of the crystalline phases. With further increase of the temperature, interactions between the molecule chains will decrease and energy transfer between the molecule chains will be lower. Hence, the value of the heat capacity of semicrystalline thermoplastics will decrease again.



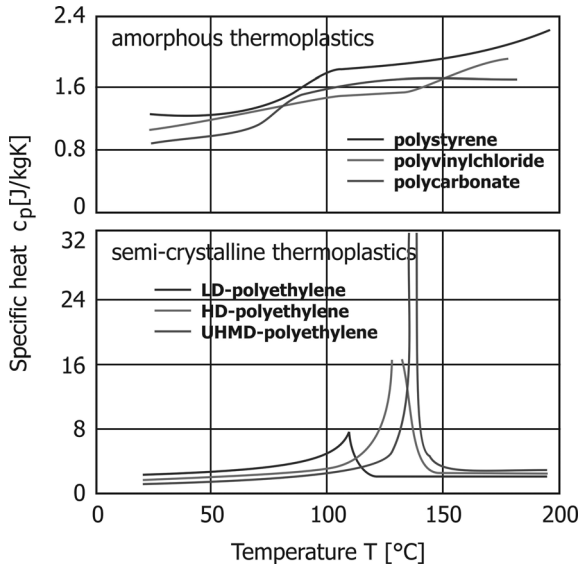


**Figure 1.24** Examples for specific heat capacity  $c_p$  of amorphous and semicrystalline thermoplastics [11].

In Figure 1.24 examples of the behavior of the heat capacity in dependence on the temperature is shown for some amorphous and semicrystalline thermoplastics [11].

### 1.3.4

#### Heat Conduction

Thermoplastics are usually electrical insulators. They have no free electrons enabling high heat conduction like for metals. Heat conduction in thermoplastics will only be done by spreading through elastic oscillations of chain segments. According to Debye [28] a relationship between heat conduction and spreading of elastic oscillations can be described by Equation 1.4.

$$\lambda = K \cdot \rho \cdot c \cdot u \cdot l \quad (1.4)$$

$K$ : dimensionless constant  $\sim 1/3$

$\rho$ : density

$c$ : heat capacity

$u$ : transmission speed for elastic oscillations

$l$ : free length of elastic oscillations.

The free length  $l$  of elastic oscillations is, for amorphous thermoplastics, of the order of the atomic distance. The transmission speed  $u$  for elastic oscillations corresponds to the speed of sound within the material. The type of bonding between

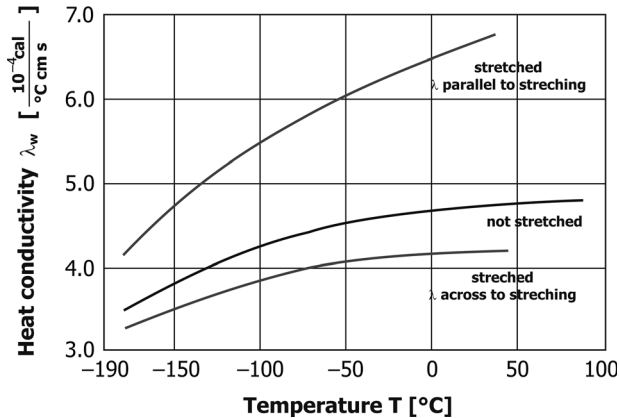


**Figure 1.25** Heat conductivity as function of the temperature for nonstretched and stretched by 375% PMMA. For the stretched material the heat conductivity is given parallel to and across the stretching direction [30].

atoms or molecule segments is of importance for the quantity of the heat conductivity. Due to covalent bonding within a macromolecule the heat conduction is 10 times higher than by essentially van der Waals bonding between the macromolecules [29].

By measuring the heat conductivity on stretched thermoplastics the influence of the bonding type can be demonstrated [23]. Stretching the material in one direction causes a stretching and an orientation of the macromolecules to one another. In the direction of stretching covalent bonding is predominant, while vertical to the stretching van der Waals bonding will be the dominant bonding type. Hence, the heat conduction will be anisotropic for stretched thermoplastics.

Figure 1.25 shows the heat conductivity on stretched and unstretched PMMA as examples. For stretched PMMA the heat conductivity is given separately parallel to and across the direction of stretching [30]. Parallel to the stretching direction the heat conductivity is higher than for not stretched material. Across the stretching direction the heat conductivity is less than for unstretched material.

The dependence on temperature of the heat conductivity is different for amorphous and semicrystalline thermoplastics. For amorphous thermoplastics in the glass state at moderate to low temperatures the temperature dependence of the heat conductivity is not really significant (see Figure 1.26). The observed increase of the heat conductivity on increasing temperature is here essential given by an increasing specific heat [31]. The material history and the measurement technique for recording the heat conductivity depending on the temperature will give nonuniform results for the course of the heat conductivity at higher temperatures for amorphous thermoplastics. In comparison to semicrystalline thermoplastics amorphous thermoplastics show, however, a clearly lower temperature dependence. Figure 1.26 demonstrates the temperature behavior of the heat conductivity for some amorphous and semicrystalline thermoplastics [6].

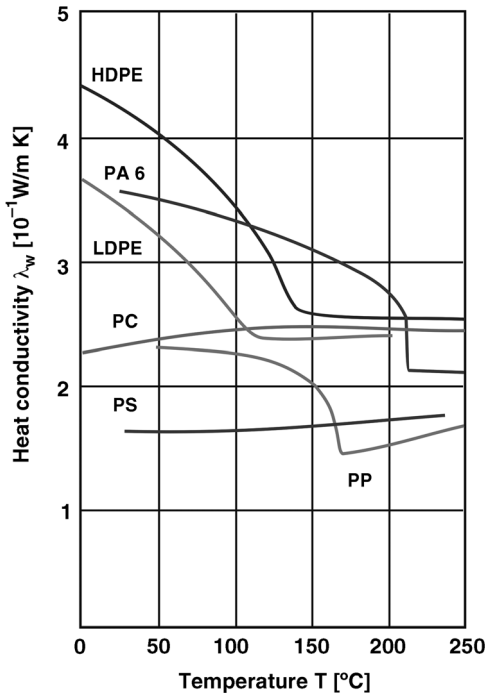


**Figure 1.26** Heat conductivity for amorphous (PC, PS) and semicrystalline thermoplastics (HDPE, LDPE, PA6 and PP) [11].

The heat conductivity of semicrystalline thermoplastics depends on the crystallization level of the material. Increasing crystallization level causes increasing density of the material, which results in a more intense heat conductivity (Figure 1.27).

A semicrystalline thermoplastic can be considered as a biphasic system, composed from amorphous and crystalline phases. The total heat conductivity  $\lambda$  of the amorphous and crystalline partition can be calculated in accordance with the composition formula (1.5) [6]:

$$\lambda = \frac{2\lambda_a + \lambda_c + 2\gamma_c(\lambda_c - \lambda_a)}{2\lambda_a + \lambda_c - \gamma_c(\lambda_c - \lambda_a)} \lambda_a \quad (1.5)$$

$\lambda_a$ : heat conductivity of amorphous phase

$\lambda_c$ : heat conductivity of crystalline phase

$\gamma_c$ : volume partition of crystalline phase.

Figure 1.28 shows schematically the contribution of amorphous and crystalline phases to the heat conductivity as a function of the temperature. For the given course of the heat conductivity  $\lambda_c$  of the crystalline phase different temperature proportionalities are valid, caused by the average free path length for elastic oscillations (see Equation 1.4) depending on the temperature [31].

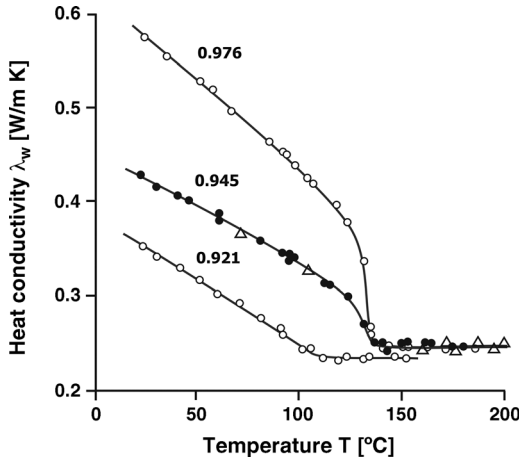


**Figure 1.27** Influence of the crystallization level to the heat conductivity of PE. Parameter of the graph is the materials density, caused by the crystallization level [6].

Up to the glass temperature  $T_g$  of the material the dependence of the heat conductivity from the temperature has a proportionality of  $1/T$ . On reaching the crystallite melting temperature  $T_m$  the near order of the crystalline phases will be broken up and the heat conductivity  $\lambda_c$  of the crystalline phases will decrease to the value of the heat conductivity  $\lambda_a$  of the amorphous phase.

### 1.3.5

#### Temperature Conduction

An important factor for a thermal processing of thermoplastics is the spreading speed of a temperature change within the material. A temperature difference  $\Delta T$  in a solid material causes a heat flux  $j$  from a warm to a cold segment (see Figure 1.29) [6]:

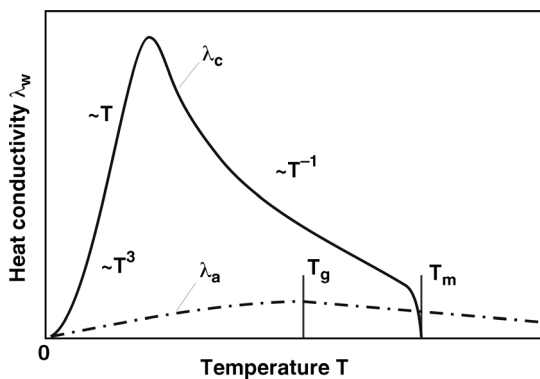


**Figure 1.28** Schematic diagram of the heat conductivity in amorphous and crystalline phases of a semicrystalline thermoplastic [31].

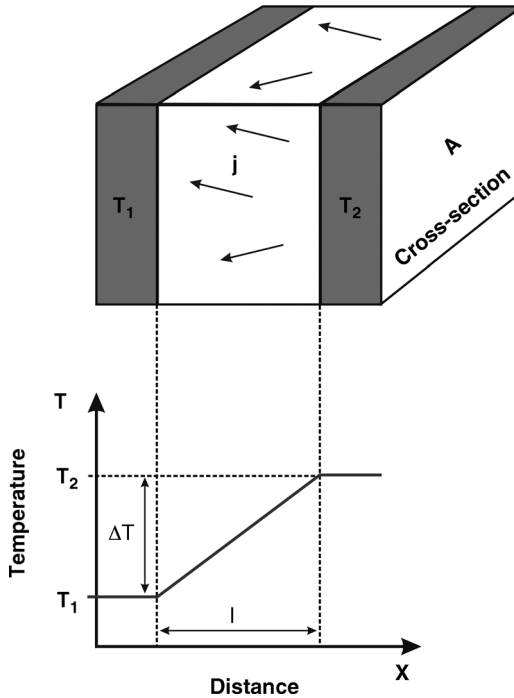


Figure 1.29 Heat transfer through a material cross section under stationary heat flux [6].

$$j = -\lambda \cdot \text{grad}(T) \quad (1.6)$$

$j$ : heat flux

$\lambda$ : specific heat conductivity.

Under stationary conditions the heat flux  $j$  is given by the quantity of heat  $\Delta Q$ , which will pass a material segment of cross section  $A$  and length  $l$  in a time interval  $\Delta t$  from the warm segment ( $T_2$ ) to the cold one ( $T_1$ ):

$$\frac{1}{A} \cdot \frac{\Delta Q}{\Delta t} = -\lambda \cdot \frac{T_2 - T_1}{l} \quad (1.7)$$

$A$ : cross section of a material segment

$\Delta Q$ : quantity of heat

$\Delta t$ : time interval

$\lambda$ : specific heat conductivity

$T_1, T_2$ : temperature.

The difference of inflow and outflow heat flux ( $\text{div}(j)$ ) in connection with a change of the inner energy  $u$  per segment volume and time  $t$  corresponds to zero, because no heat energy can disappear:

$$\varrho \cdot \frac{\partial u}{\partial t} + \operatorname{div}(j) = 0 \quad (1.8)$$

$\varrho$ : specific density

$u$ : inner energy

$t$ : time

$j$ : heat flux.

The inner energy  $u$  changes with temperature  $T$  according:

$$\partial u = c \cdot dT \quad (1.9)$$

$c$ : specific heat capacity.

Combination of Equations 1.8 and 1.9 results in the heat conduction Equation 1.10:

$$\operatorname{div}(\lambda \cdot \operatorname{grad}(T)) = \varrho \cdot c \cdot \frac{\partial T}{\partial t} \quad (1.10)$$

By the assumption of a place-independent specific heat conductivity  $\lambda$ , Equation 1.11 results from Equation (1.10):

$$\frac{\lambda}{c \cdot \varrho} \cdot \operatorname{div}(\operatorname{grad}(T)) = \frac{\partial T}{\partial t} \quad (1.11)$$

and hence the temperature conductivity  $a$ , built by the quotient of the heat conductivity  $\lambda$  with the heat capacity  $c$  and the specific density  $\varrho$  of the material:

$$a = \frac{\lambda}{c \cdot \varrho} \quad (1.12)$$

The temperature conductivity has the dimension cross section  $A$  per time interval  $t$  and describes the speed of a temperature change for heat conduction processes. A change of temperature occurs faster the higher the heat conductivity and the lower the specific heat and specific density of the material are.

Because heat conductivity, specific heat and specific density depend on the temperature, the temperature conductivity has a complex temperature dependence for amorphous and semicrystalline thermoplastics:

### 1.3.5.1 Amorphous Thermoplastics

- Heat conductivity shows a gentle rise with increasing temperature.
- Heat capacity increases on rising temperature. At the glass-transition temperature the increase is more distinctive.
- Specific density decreases slowly below the glass-transition temperature. Exceeding the glass-transition temperature the decrease is more intensive with increasing temperature.

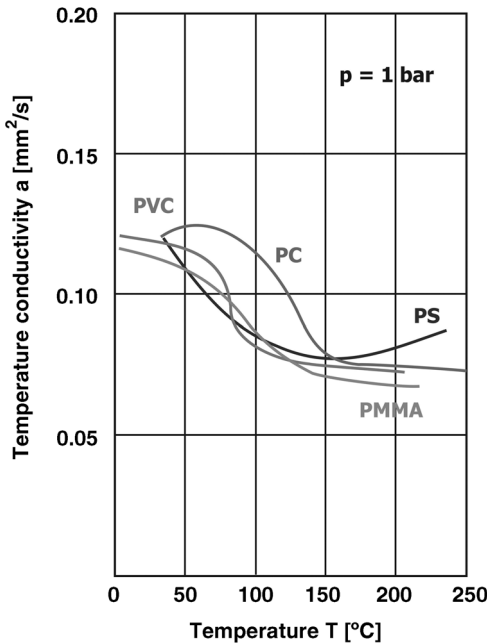


**Figure 1.30** Temperature conductivity as a function of the temperature for some amorphous thermoplastics [11].

The superposition of these effects results in a slow decrease of the temperature conductivity in the state of application by increasing temperature. At the glass-transition temperature the decrease is stronger. On increasing plasticization of the material the temperature conductivity again decreases slowly. Figure 1.30 shows the temperature dependence of the temperature conductivity for some amorphous thermoplastics [11].

### 1.3.5.2 Semicrystalline Thermoplastics

- Heat conductivity decreases noticeably up to the crystallite melt temperature. On exceeding the crystallite melt temperature the heat conductivity shows a slow increase.
- Heat capacity increases on rising temperature. At the crystallite melt temperature the heat capacity has a strong increase and then drops down above the crystallite melt temperature to lower values.
- Specific density has a quasilinear decrease below the glass-transition temperature of the amorphous phases. On exceeding the crystallite melt temperature a nonlinear decrease follows. If the material completely plasticizes the decrease of the specific density is again quasilinear.

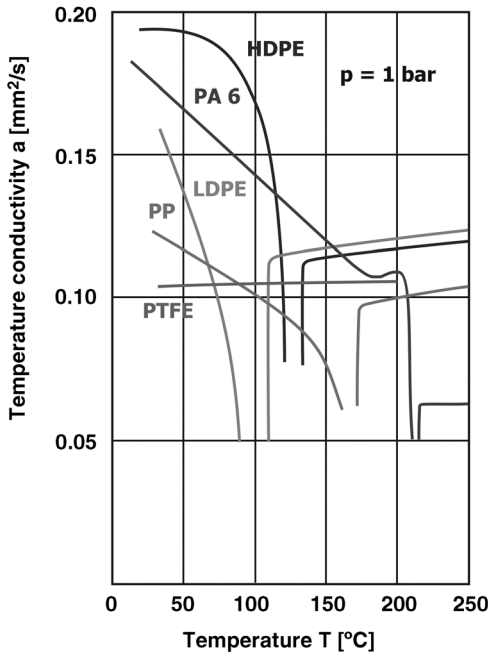


**Figure 1.31** Temperature conductivity as function of the temperature for some semicrystalline thermoplastics [11].

The temperature conductivity of semicrystalline thermoplastics is strongly dependent on the temperature of the material (Figure 1.31) caused by the superposition of the given effects. The temperature conductivity decreases on increasing temperature during the state of application and has a discontinuity at the crystallite melt temperature. Exceeding the crystallite melt temperature the temperature conductivity increases quasilinearly by increasing temperature.

Average values of the temperature conductivity for several thermoplastics are summarized in Table 1.10. As a comparison, the temperature conductivity of steel is 100 times higher than the values of thermoplastics.

**Table 1.10** Average values of temperature conductivity for some thermoplastics [32].

Resin	Temperature conductivity $a$ [ $\text{mm}^2/\text{s}$ ]
ABS	0.19
PA 6	0.05
PE	0.08
PMMA	0.17
POM	0.11
PP	0.10
PPO	0.20
SAN	0.23



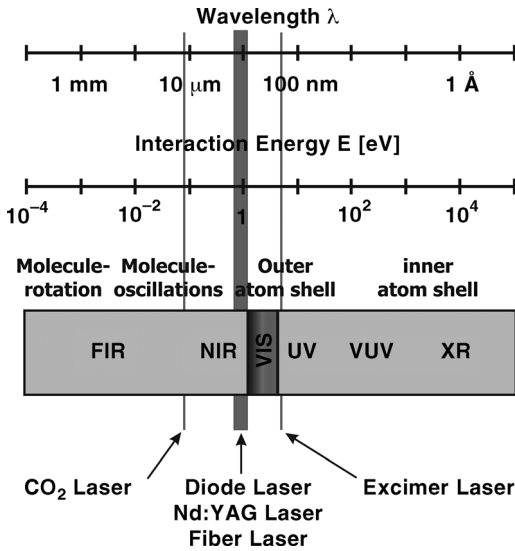


**Figure 1.32** Interaction between electromagnetic radiation and material. NIR lasers like diode, Nd:YAG or fiber lasers are in the range of electronic and starting of molecule excitation [33].

## 1.4 Optical Properties

Beside thermal properties the optical properties of thermoplastics are of importance for laser processing. The optical properties of thermoplastics without any additives like coloration dyes or reinforcement particles are influenced by the macromolecule chain structure and the type of bonding within the macromolecule chain and between the chains. The interaction of electromagnetic radiation with the material depends on the wavelength of the radiation and can be done by bonded electrons (molecule orbital) or molecule segments (Figure 1.32).

Radiation of NIR lasers like various diode lasers (e.g.,  $\lambda = 808 \text{ nm}$ ,  $940 \text{ nm}$  or  $980 \text{ nm}$ ), Nd:YAG-laser ( $\lambda = 1064 \text{ nm}$ ) or fiber lasers (e.g.,  $\lambda = 1070 \text{ nm}$  or  $1090 \text{ nm}$ ) interacts with the material by stimulating electron oscillations. Some diode and fiber lasers with wavelength between  $1.5 \mu\text{m}$  and  $2 \mu\text{m}$  interact with the material in the transition state from stimulation of electron oscillations to vibration oscillations of molecular segments. CO<sub>2</sub>-laser radiation ( $\lambda = 10.6 \mu\text{m}$ ) in the MIR spectrum induces molecular oscillations.

Because the material structure of thermoplastics is influenced by the temperature the optical properties are in principle also dependent on the temperature. Due to the complicated molecule structure of thermoplastics a theoretical analysis of the optical properties is only approximately possible.

Appropriate determination of the optical properties can be done by measurement of the reflection and transmission behavior. From the measured

reflection and transmission data the absorption property of the material can be calculated.

In this chapter the principle properties of optical constants will first be discussed. Next follows a consideration of reflection, transmission and scattering of optical radiation by thermoplastics. The absorption of radiation in pure resins in the different wavelength areas and in particular the possibilities of influencing the absorption by additives will be discussed in detail.

#### 1.4.1

##### Optical Constants

The distribution of electromagnetic waves in a solid body is described by the wave equation:

$$-\Delta E + \frac{1}{c^2} \ddot{E} = -\mu \cdot \mu_0 \cdot \ddot{P} \quad (1.13)$$

$E$ : electric field strength

$c$ : speed of light

$\mu$ : relative permeability (= 1 for insulators)

$\mu_0$ : magnetic field constant

$P$ : macroscopic polarization.

The macroscopic polarization  $P$  of the material is linked with the electric field strength of a light wave by [34]:

$$P(t) = (\hat{\epsilon} - 1) \cdot \epsilon_0 \cdot E(t) \quad (1.14)$$

$\hat{\epsilon}$ : complex dielectric constant

$\epsilon_0$ : electric field constant

$E(t) = E_0 \exp(-i(kz - \omega t))$ : electric field strength of light wave.

The macroscopic polarization  $P$  is the sum of all oscillating dipole moments  $p = q \cdot x(t)$  in the solid body:

$$P(t) = N \cdot q \cdot x(t) \quad (1.15)$$

$N$ : number of possible oscillating dipoles

$q$ : charge

$x(t)$ : oscillation amplitude.

Effecting as dipoles depending on the light wave frequency are in the NIR spectral range ( $\lambda < 2 \mu\text{m}$ ) e.g., bonded electrons or in the MIR spectral range ( $2 \mu\text{m} < \lambda < 30 \mu\text{m}$ ) charge distributions of macromolecule chain segments. Oscillations of such dipoles can be stimulated by the electric field of the light wave. The oscillation amplitude  $x(t)$  of the oscillating components is given by the solution of the wave equation:

$$\ddot{x} + \gamma \dot{x} + \xi x = \frac{q}{m} \cdot E(t) \quad (1.16)$$

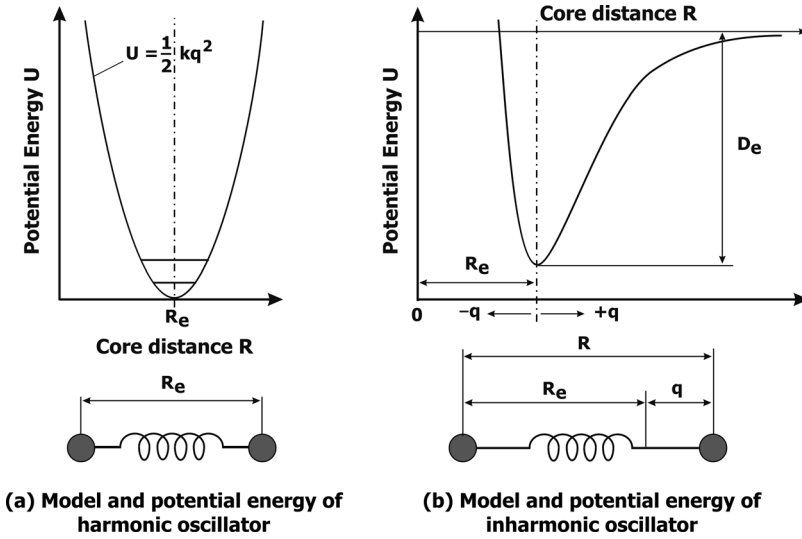


**Figure 1.33** Potential-energy course of harmonic (a) and inharmonic (b) oscillator [35]. The term  $q$  is used for the mass elongation out of the balance position.

$\gamma$ : damping constant

$\xi$ : spring constant.

The second term of Equation 1.16 describes the speed-dependent damping of the oscillation. The third term gives the bonding force for the oscillating system.

In the case of low oscillation amplitudes the bonding force is proportional to the elongation (harmonic oscillator). For high oscillation amplitudes the bonding force tends to zero and the oscillating system will break up. In this case, the theoretical model of the oscillating system has to be replaced by the model of an inharmonic oscillator (Figure 1.33) [35]. As an approximation, the following considerations will be restricted to the case of low oscillation amplitudes.

Attempting the harmonic oscillator model the general solution of the oscillation Equation 1.16 results in the amplitude  $x(t)$ :

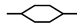
$$x(t) = \frac{q \cdot E(t)}{m(\omega_0^2 - \omega^2) + i\gamma\omega} \quad (1.17)$$

Using Equation 1.15 the macroscopic polarization Equation 1.14 results in:

$$P(t) = N \cdot \frac{q^2}{m} \cdot \frac{E(t)}{(\omega_0^2 - \omega^2) + i\gamma\omega} \quad (1.18)$$

Equation 1.18 is valid for a single resonance oscillation of a dipole system. For an expansion to all possible resonance oscillations of the system the sum over all oscillation numbers has to be made, regarding the connection strength. For atomistic systems this will be summarized by the optical polarization  $\hat{a}$  [36]:

**Table 1.11** Molecule groups of polymer materials and their mol refraction [37].

Molecule group	Mol refraction $P_m$ ( $\times 10^{-16}$ [ $C^2 m^2/J$ ])
$-CH_3$	6.20
$-CH_2-$	5.01
$>CH-$	3.98
$>CH<$	2.84
	27.5
$-O-$	5.72
$>C=O$	11.0
$-CO_2-$	16.5
$-CONH-$	33.0
$-O-CO_2-$	24.2
$-S-$	8.80
$-F$	1.98
$-Cl$	10.45
$-C\equiv N$	12.1
$-CF_2-$	6.88
$-CCl_2-$	19.47
$-CHCl-$	13.7

$$P(t) = \hat{a} \cdot N \cdot E(t) \quad (1.19)$$

For molecular systems like polymeric materials the optical polarization  $\hat{a}$  will be replaced by the mol refraction  $\hat{P}_m$ . The mol refraction indicates the ability of molecules to become polarized. The polarization of the monomer unit of a macromolecule is also valid in sum for the entire macromolecule [37]. The optical polarization  $\hat{a}$  is linked with the mol refraction  $\hat{P}_m$  by the molecular weight  $M$  of the monomer unit and the specific volume  $V$  of the polymeric material [36]:

$$\hat{a} = \frac{1}{N} \cdot \frac{\hat{P}_m}{M \cdot V} \quad (1.20)$$

$\hat{a}$ : complex optical polarization

$\hat{P}_m$ : mol refraction of one monomer unit

$M$ : molecular weight of monomer unit

$V$ : specific volume of polymer.

Table 1.11 gives some examples of molecule groups and values of their mol refraction (from [37]).

The wave Equation 1.13 results in Equation 1.21, inserting Equations 1.18 and 1.19 by using  $\mu_0 \epsilon_0 = c^{-2}$ :

$$-\Delta E + \frac{1}{c^2} \cdot \left( 1 + \frac{1}{\epsilon_0} \cdot \frac{\hat{P}_m}{M \cdot V} \right) \cdot \ddot{E} = 0 \quad (1.21)$$

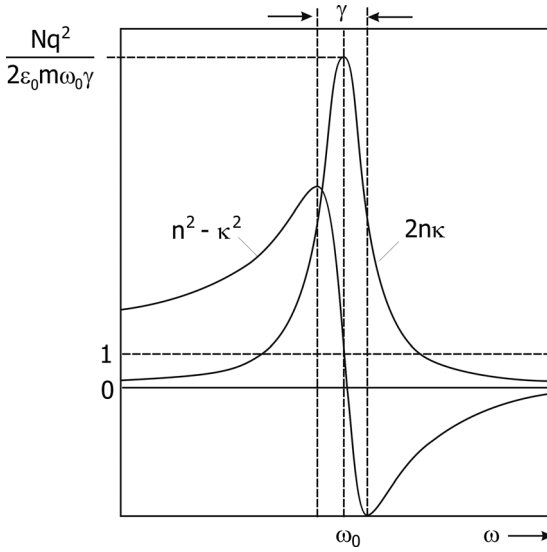


**Figure 1.34** Schematic course of Equations 2.23a, b around a resonance frequency  $\omega_0$  [38].

Using the solution attempt of plane waves for the electrical field of a light wave, the complex refractive index of the material results in:

$$\hat{n}^2 = 1 + \frac{1}{\varepsilon_0} \cdot \frac{\hat{P}_m}{M \cdot V} \quad (1.22)$$

$$\hat{n}^2 = k^2 c^2 / \omega^2: \text{ complex refractive index } (\hat{n} = n - i\kappa)$$

Dividing into real and imaginary parts of the complex refractive index around a resonance point will give by using Equation 1.17:

$$n^2 - \kappa^2 = 1 + \frac{N \cdot q^2}{\varepsilon_0 \cdot m} \cdot \frac{\omega_0^2 - \omega^2}{(\omega_0^2 - \omega^2)^2 + \gamma^2 \cdot \omega^2} \quad (1.23a)$$

$$2n \cdot \kappa = \frac{N \cdot q^2}{\varepsilon_0 \cdot m} \cdot \frac{\gamma \cdot \omega}{(\omega_0^2 - \omega^2)^2 + \gamma^2 \cdot \omega^2} \quad (1.23b)$$

Figure 1.34 shows the schematic course of Equations 1.23a and 1.23b around a resonance point.

The imaginary part Equation 1.23b tends to zero outside the resonance and from Equation 1.23a follows for the real refractive index by using the mol refraction according to the Lorentz–Lorenz law [36]:

$$n = \sqrt{1 + \frac{3 \cdot P_m}{M \cdot V \cdot P_m}} \quad (1.24)$$

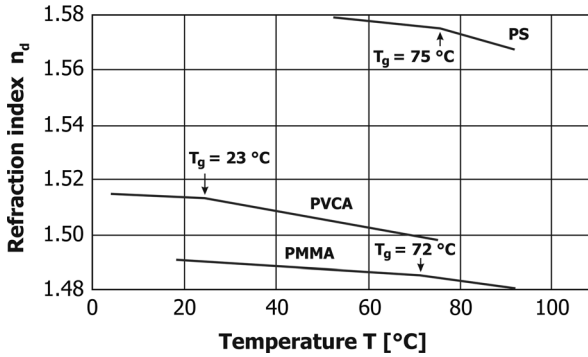


Figure 1.35 Temperature dependency of the refractive index for PMMA, PS and PVCA [40].

By the assumption of temperature independence for mol refraction and molecular weight, the temperature dependence of the specific volume of the polymeric material will influence the temperature dependence of the refractive index. Usually, the specific volume will increase on increasing temperature [39], which results in a decrease of the refractive index on increasing temperature.

Figure 1.35 shows for some polymers the course of the refractive index as a function of the temperature, calculated by Equation 1.24 with regard to the temperature-dependent specific volume. On reaching the glass temperature of the polymer the course of the refractive index shows a bend. This is given by a rapid increase of the specific volume, caused by increased mobility of the molecule chains [6].

At the maximum of the resonance the frequency of the wave is  $\omega = \omega_0$ . Using Equation 1.23b the absorption constant  $\kappa$  is given by:

$$\kappa = \sqrt{\frac{N \cdot q^2}{2 \cdot \epsilon_0 \cdot m \cdot \omega_0 \cdot \gamma}} \quad (1.25)$$

$N$ : number of oscillators

$q$ : electric charge

$\epsilon_0$ : dielectricity constant

$m$ : mass

$\gamma$ : damping constant.

The line width of a resonance in a solid body is dependent on the density distribution of the absorption spots, the damping strength for the forced oscillation and the influence on the oscillation by connection with further oscillation-capable components of the material. In polymeric materials the absorption line course is determined by the inhomogeneous line spreading. The course of the line can be described by the Gauß line spreading (Figure 1.36) [41].

$$\kappa_\nu = \kappa_0 \cdot \frac{2\sqrt{\ln 2}}{\pi(\Delta\nu_0)} \cdot \exp\left(-4 \cdot \ln 2 \cdot \frac{(\nu - \nu_0)^2}{(\Delta\nu_0)^2}\right) \quad (1.26)$$

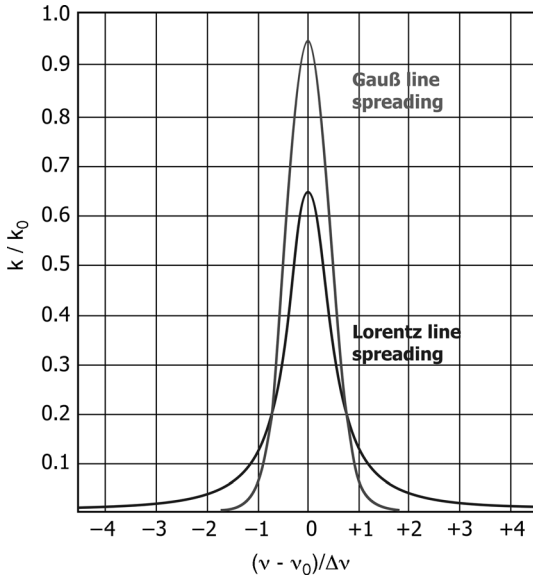


**Figure 1.36** Schematic sketch of Gauß and Lorentz line spreading [41], shown is the normalized wave number  $k/k_0$  as function of the frequency difference  $\nu - \nu_0$  in regard to the line width.

$\nu$ : frequency

$\nu_0$ : resonance frequency.

The line spreading results from the statistical surrounding of the molecule chains, which causes a resonance frequency shift of the oscillation modes of individual recurring molecule components. The shifted resonance frequencies themselves have a homogeneous line spreading, described by the Lorentz line spreading (Figure 1.36) [41]:

$$\kappa_\nu = \frac{\kappa_0 \cdot \gamma}{(\nu - \nu_0)^2 + \gamma^2/4} \quad (1.27)$$

The envelope of all resonance lines results in the inhomogeneous line spreading of the absorption spot.

As a model assumption, in areas with strong near order and regular molecular structure – as for crystalline structures – a band structure of energy levels is given for the bonding electrons within the molecule orbital that enables primarily electronic stimulation. In contrast to this in amorphous areas it is more probable that absorption of NIR-laser radiation will occur as vibration excitation caused by the statistical molecule chain order with unhindered chain components. In polymeric materials usually no resonant stimulated base oscillations are given within the NIR wavelength spectrum so absorption of such radiation can only occur by stimulation of higher-order oscillations.

Due to the complex and irregular molecule structure the energy levels of electronic and vibration oscillations of the molecule chains will be influenced by adjoining molecule chains [42] like for crystalline phases by highly orientated chains or for stretched amorphous molecule chains in stretched polymer fibers. Influencing of oscillation levels will result in a shift of the resonance frequency for the oscillation stimulation. Because the state of the molecule structure is dependent on the temperature also the influencing of the oscillation levels are dependent on the temperature. Increasing temperature affects a shift of the resonance frequencies, resulting in increasing or decreasing absorption as a function of the temperature.

Complicating the theoretical consideration is the availability of additives like filler materials, coloration dyes or reinforcement fibers that can reflect or absorb the radiation themselves.

The preceded discussion is important for the theoretical understanding of the processes during interaction of electromagnetic radiation and solid material. The following considerations will deal in more detail with the special features of the interaction with plastic material.

Starting with the macroscopic behavior, like reflection and transmission, the absorption mechanism for the wavelength areas used for laser welding plastics and internal scattering by additives in the resin will be considered.

#### 1.4.2

##### **Reflection, Transmission and Absorption Behavior**

When electromagnetic radiation hits the surface of a solid material, usually a part of the radiation will be reflected at the surface. The nonreflected part of the radiation will enter the material and can be weakened by scattering on internal elements like pigments or crystalline phases and by absorption [43]. Depending on material thickness and internal radiation loss the rest of the radiation will be transmitted (Figure 1.37).

Reflection and transmission of radiation are quantities that can be measured by spectral photometers [44]. Figure 1.38 shows as an example the reflection and transmission measurement results on PC at visible and NIR wavelengths between 400 and 2500 nm and the corresponding calculated absorption.

Absorption of electromagnetic radiation in an electric insulating material is done by stimulation of dipole oscillations [45]. Depending on the frequency, induced or permanent dipoles are given by for example, bonded electrons for NIR radiation ( $\lambda < 2000$  nm) or charge distributions of molecule segments from macromolecules for IR radiation ( $2 \mu\text{m} < \lambda < 30 \mu\text{m}$ ).

From measured reflection and transmission data the radiation loss by absorption in the material can be calculated (see Figure 1.38). If necessary, the influence of internal scattering has to be taken into consideration.

The energy balance of the radiation in principle will have no losses during pure scattering, whereas by absorption the radiation energy will be transformed into



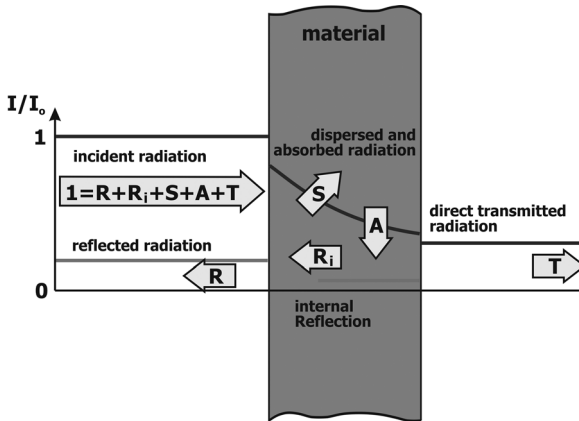


**Figure 1.37** Radiation intensity weakening by reflection as well as internal scattering and absorption during passing material.

another energy state like heat energy as induced molecule motion. Under the assumption of linear absorption mechanism the reduction of the radiation intensity can be described by the Lambert absorption rule [36]:

$$I_T(z) = I_0 \cdot \exp\left(-\frac{4 \cdot \pi \cdot \kappa}{\lambda} \cdot z\right) \quad (1.28)$$

$z$ : material thickness

$\alpha = 4\pi\kappa/\lambda$ : absorption constant.

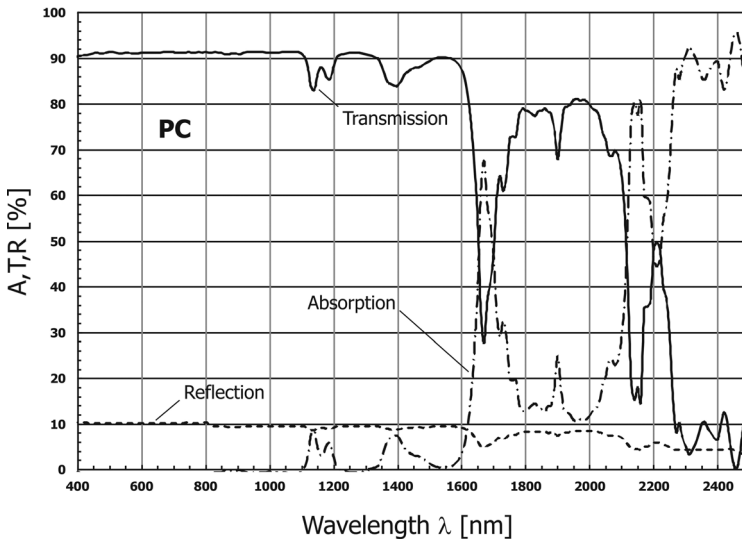


**Figure 1.38** Reflection, transmission and absorption of PC at wavelengths between 400 and 2500 nm.

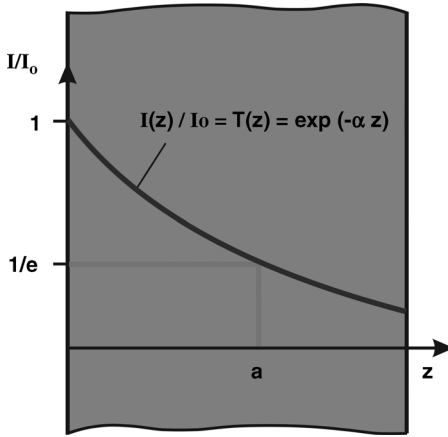


**Figure 1.39** Exponential decrease of radiation intensity in a material, described by the Lambert absorption rule.

The Lambert absorption rule indicates that by increasing material thickness  $z$  the transmitted radiation will decrease exponential (Figure 1.39). Within every differential layer  $\delta z$  of the material the same fraction of the radiation will be absorbed [36].

The absorption constant  $\alpha = 4\pi\kappa/\lambda$  in Equation 1.28 is generally correlated with the radiation wavelength  $\lambda$  and the material properties, which are summarized in the absorption coefficient  $\kappa$ . The absorption constant has the dimension of a reciprocal length (e.g., 1/mm).

In ratio to the incident radiation intensity  $I_0$  the radiation intensity  $I_T$  at the optical penetration depth ( $z = a$ ) within the material is decreased by the value  $1/e$  (Figure 1.39):

$$\frac{1}{e} = \frac{I_T(a)}{I_0} = \exp(-\alpha \cdot a) \quad (1.29)$$

By reciprocal and logarithm calculation it results from Equation 1.29:

$$\ln e = 1 = \alpha \cdot a \quad (1.30)$$

and therefore

$$\alpha = \frac{1}{a} \quad (1.31)$$

The quantity  $a$  in Equation 1.31 has the dimension of a length (e.g., mm) and defines the optical penetration depth of the material as a measure for the absorption property of the material for a specific wavelength.

Inserting Equation 1.31 into Equation 1.28 results in:

$$I_T(z) = I_0 \cdot \exp\left(-\frac{z}{a}\right) \quad (1.32a)$$

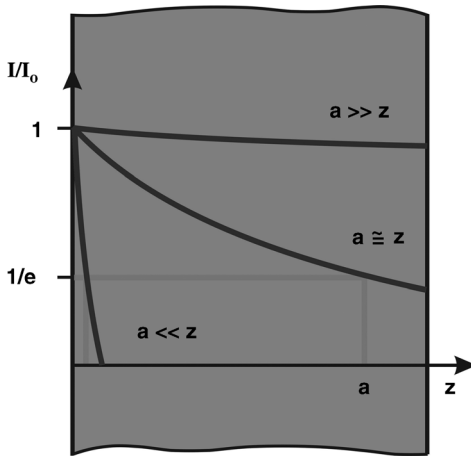


**Figure 1.40** State distinction for the ratio of optical penetration depth  $a$  to the material thickness  $z$ .

Dividing Equation 1.32a by the incident radiation intensity  $I_0$  will give the transmitted radiation  $T(z)$ , which is a measurable quantity:

$$\frac{I_T(z)}{I_0} = T(z) = \exp\left(-\frac{z}{a}\right) \quad (1.32b)$$

Further transformation by logarithm and reciprocal computation and clearing up the optical penetration depth will give a term that can be used for calculation of the optical penetration depth by the well-known thickness of the work piece and the measured transmission value:

$$a = -\frac{z}{\ln T(z)} \quad (1.32c)$$

Using the optical penetration depth  $a$  in correlation with the work piece thickness  $z$  the absorption behavior of a material can be classified for the given wavelength of the radiation (Figure 1.40):

- $a \gg z$ : the material is transparent to the radiation,
- $a \approx z$ : the radiation will be absorbed in the volume,
- $a \ll z$ : the radiation will be absorbed at the material surface.

An example of surface and volume absorption of laser radiation with a natural plastic is given in Figure 1.41 for a  $\text{CO}_2$  (left) and Nd:YAG laser (right) on PA6 with a sample thickness of 2 mm [46]. In both cases the same laser power (50 W) and processing speed (100 mm/s) was used for processing.

At PA6 the  $\text{CO}_2$ -laser radiation at  $\lambda = 10.6 \mu\text{m}$  has an optical penetration depth of approximately  $60 \mu\text{m}$ , much smaller than the material thickness. The radiation was absorbed at the surface of the PA6 sample and essentially sublimated the resin material; a molten layer of a thickness of the optical penetration depth can be seen.

In the same resin Nd:YAG-laser radiation at  $\lambda = 1.06 \mu\text{m}$  has an optical penetration depth of around 3 mm, which is of the order of the sample thickness. The Nd:YAG-

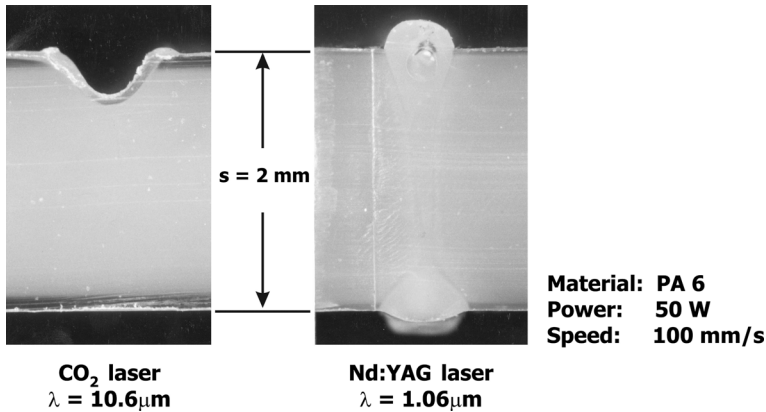


**Figure 1.41** Influence of the optical penetration depth to the processing result on PA6 using CO<sub>2</sub>- and Nd:YAG-laser radiation with the same processing parameters [46].

laser radiation was absorbed in the volume and the sample is melted through, supported by the transmitted radiation backscattered from the aluminum plate.

Table 1.12 gives the optical penetration depth for CO<sub>2</sub>-laser radiation and diode laser radiation ( $\lambda = 940 \text{ nm}$ ) for some typical natural plastics. The given values show very clearly that CO<sub>2</sub>-laser radiation is usually absorbed at the resin surface while diode-laser radiation will transmit the material with no effective absorption.

### 1.4.3

#### Scattering of NIR- and IR-Radiation in Plastics

Beside absorption an intensity loss (not an energy loss) of the incident radiation within the plastic can occur by scattering caused by inhomogeneous structures in the material.

In polymeric material, scattering of radiation can be caused by the structure of the macromolecules by themselves, on crystalline phases incorporated in the amorphous

**Table 1.12** Optical penetration depth of some typical thermoplastic resins for CO<sub>2</sub>- and diode-laser radiation.

Resin	$a \text{ [mm]} \lambda = 940 \text{ nm}$	$a \text{ [mm]} \lambda = 1064 \text{ nm}$	$a \text{ [mm]} \lambda = 1550 \text{ nm}$	$a \text{ [mm]} \lambda = 10.6 \mu\text{m}$
Amorphous Thermoplastics				
PC	22.82	23.04	18.94	0.070
PMRA	37.93	36.56	22.10	—
PVC	—	—	—	0.020
Semicrystalline Thermoplastics				
LDPE	8.49	10.34	9.71	0.280
PA 6	5.06	5.06	3.01	0.040
PP	11.63	12.87	12.96	0.190

phase [47] as well as by filler materials, fibers or coloration pigments incorporated in the polymeric matrix [48]. The kind of scattering is correlated with the wavelength of the radiation and the size of the dispersing structure [49]. Additionally, the scattering structures can themselves absorb the radiation.

Generally, for scattering in correlation with the structure size  $l$  and the wavelength  $\lambda$  following case distinctions can be made [43]:

- I:  $l \gg \lambda$ : diffraction on microscopic structures,
- II:  $l > \lambda$ : Mie scattering on statistic distributed scattering structures,
- III:  $l \ll \lambda$ : Rayleigh scattering, Raman scattering.

Under the assumption of intensity independence, weakening of the radiation intensity by scattering can be described by the exponential rule of Lambert [50]:

$$I_s = I_0 \cdot \exp(-K^+ \cdot z) \quad (1.33)$$

- $I_s$ : decreased scattering intensity
- $K^+$ : scattering constant
- $z$ : material thickness.

For spherical scattering structures with dimension smaller than the wavelength (Rayleigh scattering) the scattering constant is depending on the number  $N$  and the volume  $V$  of the particles as well as from the wavelength of the radiation [50]:

$$K^+ = -\frac{N \cdot V^2}{\lambda^4} \quad (1.34)$$

- $N$ : number of scattering structures
- $V$ : volume
- $\lambda$ : wavelength.

For large dimension of the spherical scattering structures versus the wavelength (diffraction on microscopic structures), the scattering constant is proportional to the sum of the cross-sectional areas of the particles:

$$K^+ = -\pi \sum_1^N Q_i^2 \quad (1.35)$$

- $Q_i$ : Scattering cross section of particle  $i$ .

Thus, it is assumed that the scattering structures have no interaction between themselves.

Figure 1.42 shows a graphical portrayal, taken from [50], of the spherical structure scattering constant at low particle concentration as a function of the radiation wavelength.

The relationship of the scattering constants given in Equations 1.34 and 1.35 as well as the graphical portrayal in Figure 1.42 are only valid for spherical scattering structures. They are a simple assumption with regard to realistic geometries of particles in the resin. The mathematical link between scattering constants and geometrical structure of structures like molecule chains, crystalline phases or filler

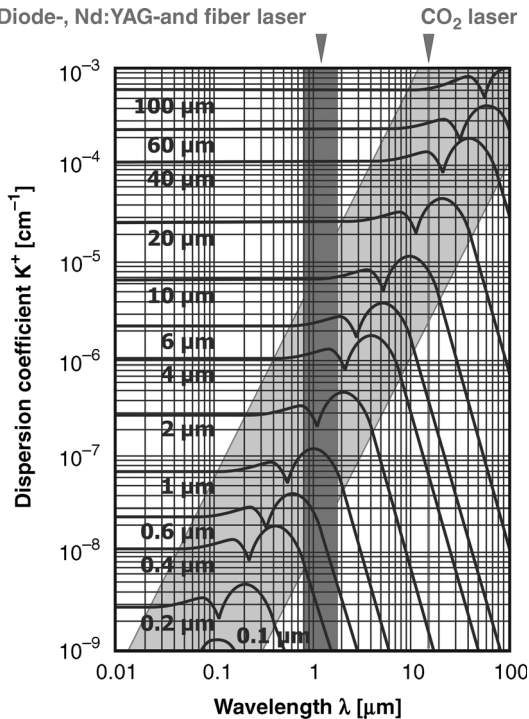


**Figure 1.42** Calculated scattering coefficient of spherical particles as function of the wavelength. The parameter of the individual graphs is the radius of the particles [50].

materials is considerably more complex [49]. For a simple assessment of the scattering influence the consideration of spherical scattering structures is sufficient. To carry out a quantitative analysis of the scattering constants the real geometric structures have to be taken into consideration.

Table 1.13 gives a summary of possible scattering structures in polymers and their dimensions. The comparison of the dimension with the wavelength of NIR radiation (e.g., diode, Nd:YAG and fiber lasers) as well as MIR radiation (e.g., CO<sub>2</sub> laser) results in a selection of the effective scattering processes.

Scattering caused by the polymer matrix corresponds to Rayleigh scattering and is proportional to  $\lambda^{-4}$ . Thus, scattering of CO<sub>2</sub>-laser radiation is by a factor  $10^{-4}$  lower than for Nd:YAG-laser radiation. In principle, scattering by the polymer matrix can be neglected for application of CO<sub>2</sub>-laser radiation.

For filler materials and pigments the scattering is dependent on the particle size. In this case, diffraction on microscopic structures and Rayleigh-scattering is predominant (see Table 1.13). For diffraction on microscopic structures the dependence is given by the particle size and not by the wavelength. The influence of the scattering caused by filler materials or pigments on the decrease of the radiation intensity in the polymer material always has to be considered in correlation with the absorption by the base material.

**Table 1.13** Dimension of scattering structures in polymers and their effect to NIR and MIR radiation [51, 52].

Structure	Dimension	Dispersion process	
		NIR radiation for example, $\lambda = 1.06 \mu\text{m}$	MIR radiation for example, $\lambda = 10.6 \mu\text{m}$
Polymer matrix:			
Crystallites	about 10 nm	III	III
Spherulithes	30–40 nm	III	III
Filler materials:			
Asbestos flour	20–80 nm	III	III
Calcium carbonate	4–25 $\mu\text{m}$	II	II
Glimmer	20–80 nm	III	III
Wood flour	<200 $\mu\text{m}$	I	I–II
Microglass spheres	5–50 $\mu\text{m}$	I–II	II
Color pigments	0.01–1 $\mu\text{m}$	II–III	III
Quartz flour	16–300 $\mu\text{m}$	I	I–II
Carbon particles	10–120 $\mu\text{m}$	I	I–II
Slate flour	<100 $\mu\text{m}$	I	I–II
Fiber materials:			
Aramid fibers	$\phi$ about 10 $\mu\text{m}$	I	II
Cellulose fibers	l about 220–650 $\mu\text{m}$	I	I
	$\phi$ about 20–25 $\mu\text{m}$	I	I–II
Carbon fibers	$\phi$ about 10 $\mu\text{m}$	I	II
Short glass fibers	l about 140–300 $\mu\text{m}$	I	I
	$\phi$ about 10–20 $\mu\text{m}$	I	II
Long glass fibers	l < 6 mm	I	I
	$\phi$ about 10–20 $\mu\text{m}$	I	II

I:  $l \gg \lambda$ : Diffraction on microscopic structures ( $K^+ \propto N \cdot Q^2$ ).

II:  $l > \lambda$ : Mie scattering on statistic distributed scattering structures.

III:  $l \ll \lambda$ : Rayleigh scattering, Raman scattering ( $K^+ \propto N \cdot \lambda^{-4}$ ).

Scattering by fiber materials will be done by diffraction and is not dependent on the wavelength. The influence of the scattering on the decrease of radiation intensity passing a material is correlated with the absorption properties of the material. For low optical penetration depths the scattering can be in principle neglected. When the optical penetration depth is in the range of mm, the scattering has to be taken into consideration.

#### 1.4.4

##### Absorption of NIR-Laser Radiation ( $\lambda = 800 \text{ nm to } 1200 \text{ nm}$ )

In the NIR wavelength range with diode lasers (e.g.,  $\lambda = 808 \text{ nm}$ ,  $940 \text{ nm}$  or  $980 \text{ nm}$ ), Nd:YAG-lasers ( $\lambda = 1064 \text{ nm}$ ) or fiber lasers (e.g.,  $\lambda = 1070 \text{ nm}$  or  $1090 \text{ nm}$ ), interaction of the radiation with the material occurs by electronic excitation of electrons in

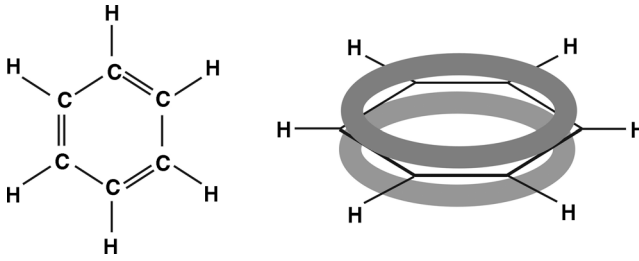


**Figure 1.43** Molecule structure (left) and molecule orbital order of the carbon valence electrons (right) for benzene.

the outer shell of atoms and by higher-order vibrational excitation of molecule segments [37] (see Figure 1.32).

In correlation with the statistical molecule structure of polymers an exact assignment of the corresponding processes for absorption of the laser radiation is not unambiguously possible [37]. For absorption of NIR laser radiation both processes have to be considered.

#### 1.4.4.1 Electronic Excitation

In polymers, the valence electrons of the individual atoms are bound in molecule orbitals of the macromolecules [53]. For covalent bonds the outer electron shells are overlapping, while the inner electrons are not significantly influenced.

An example of the placement of the carbon atom valence electrons is the benzene molecule [53] (Figure 1.43), which for example, is present in polymers like polyethylenterephthalate (PET), polycarbonate (PC) or polyphenylensulfide (PPS). The structure of a benzene molecule is given by 6 carbon atoms in a hexagonal ring with one hydrogen atom on each corner. The valence electrons of the carbon atoms form two rings as electron clouds above and below the molecule level.

At room temperature generally the valence electrons are in the basic level. Under resonant influence of electromagnetic radiation the electron energy will increase by absorption and the electrons will gain a higher energy level (Figure 1.44). According to the Born–Oppenheimer theorem [42] the level change will occur so fast that the atom nucleus can be assumed as static. The time constant for the level change is in the order of  $10^{-16}$  s [42], while atom nucleus oscillations have a time constant of  $10^{-13}$  s.

Each electron state has an own characteristic potential course for the bonding energy between electron and atom nucleus. Hence, the inharmonious of the potential curve has to be noted. Only oscillation bands occur in an absorption spectra of which the distances are specific to the oscillation states of the excited electrons. The intensities of the occurring spectral lines are correlated according to the Franck–Condon principle [42]. The level-change probability for a change from the basic level to a higher-order level is greatest for electron oscillations where the oscillation eigenfunctions at the near-nucleus and far-nucleus branches have amplitude minima for the potential curves (Figure 1.44).



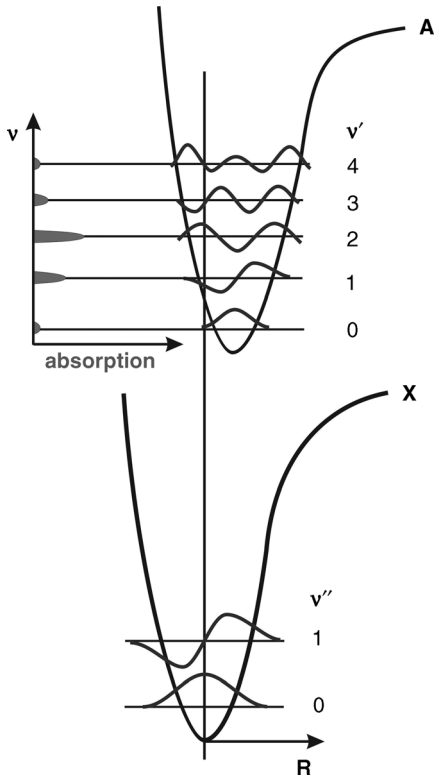


**Figure 1.44** Excitation of electronic-level change from basic level X to higher level A. According to the Franck–Condon principle the absorbed intensity is at its highest if the maxima or minima of oscillation eigenfunctions are overlapping [42].

The electron state change causes a disruption of the coulomb forces equilibrium state between the electrons and thereby a disruption of the force equilibrium state within the molecule [54]. This results in an increase of the distances of all equilibrium states and thereby in a change of the oscillation levels. The molecules will experience oscillations that will be transmitted to the rest of the molecule chain. This process will generate a transformation of electromagnetic radiation into thermal oscillation energy of the molecule chains.

#### 1.4.4.2 Vibronic Excitation

In polymers, components of the macromolecular chains can oscillate in different ways like elongation, bending or rotating oscillation. Such oscillations can be induced by absorption of electromagnetic radiation when resonant wavelengths are available. For NIR radiation usually no resonant base oscillations can be stimulated. But influence by electromagnetic radiation can stimulate higher-order oscillations with lower oscillation frequencies than the base oscillation [55]. The intensity of higher-order oscillations is noticeably reduced compared with the base oscillation [56]

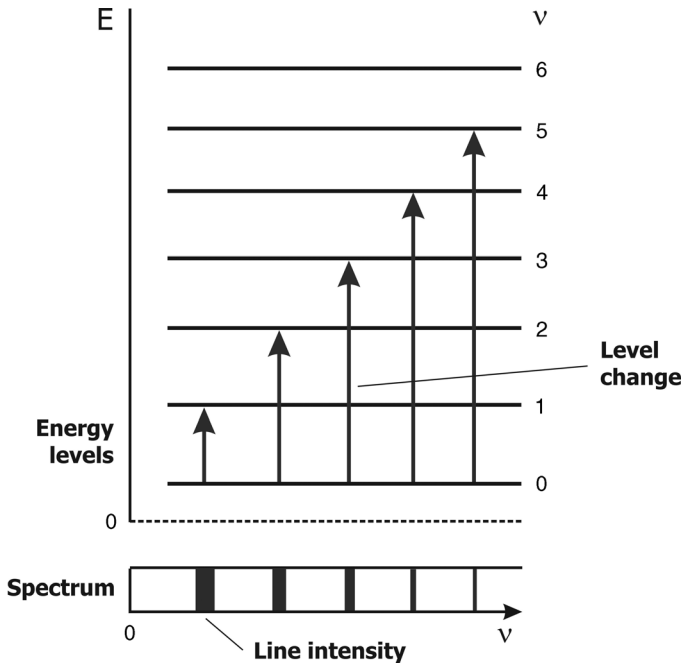


**Figure 1.45** Schematic portrayal of absorbed radiation intensity for base and higher-order oscillations caused by vibronic excitation [56].

(Figure 1.45), which caused an increased optical penetration depth for absorption of electromagnetic radiation by vibronic excitation in natural polymers.

An example of absorption of NIR radiation is the stimulation of third-order vibronic oscillation of the CH valence oscillation with a base oscillation frequency of  $\nu = 3100 \text{ cm}^{-1}$  [55] corresponding to a wavelength of  $\lambda = 3.23 \text{ }\mu\text{m}$ .

#### 1.4.4.3 Summarizing Comment

In a regular structured material like metals or semiconductors, caused by the crystalline structure, a distinctive electronic band structure exists that is responsible for an effective absorption of NIR radiation. In contrast to this, in a natural polymeric material only statistically distributed molecule segments exist that can have an electronic band structure. Electronic as well as vibronic oscillation excitation, also higher-order vibronic excitation, occurs only with minor quantum effectiveness. Hence, an effective absorption of NIR radiation between 800 and 1200 nm on natural polymers is of little value. Figure 1.46 shows as an example the directed transmission for PC, PMMA and PP in the wavelength range from 800 to 1200 nm.

While the incident radiation is nearly completely transmitted by the amorphous plastics PC and PMMA, the semicrystalline PA6 and PP show a decrease of the radiation by scattering on crystalline structures. This indicates not an effective absorption of the radiation but a decrease of the radiation intensity by scattering.

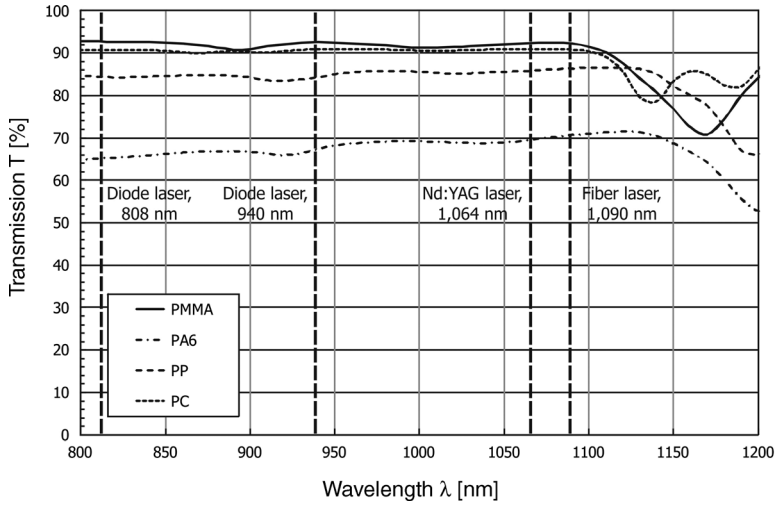


**Figure 1.46** Transmission of PA6, PC, PMMA und PP in the wavelength range from 800 to 1200 nm (sample thickness 2 mm).

An example of this shows the transmission measurement on semicrystalline PA6, carried out with low-power Nd:YAG-laser radiation (Figure 1.47). The radiation is noticeably dispersed by the semicrystalline structure of the 4-mm thick PA6 sample but not absorbed. Using for comparison a mostly amorphous and optically clear PA6 film the transmission measurement results in an optical penetration depth of

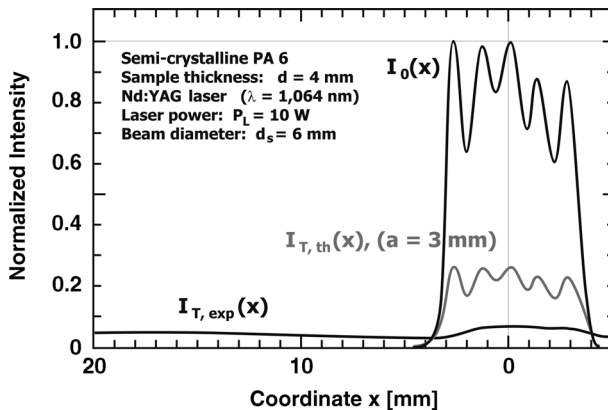


**Figure 1.47** Transmission measurement on a 4-mm thick semicrystalline PA6 sample using a Nd:YAG laser. Given is the measured intensity distribution without  $I_0(x)$  and with the sample

$I_{T,exp}(x)$ . For comparison the calculated transmitted intensity distribution  $I_{T,th}(x)$  of a 4-mm thick amorphous PA6 sample is given (marked green) [57].

**Table 1.14** Characteristic C–H group oscillations in the wavelength range between 1200 and 2500 nm [59].

Oscillation type of C–H group	Wave number range [ $\text{cm}^{-1}$ ]	Wavelength range [nm]
Combination oscillation	4500–4200	2220–2380
First high-order oscillation, stretching oscillation	5600–6200	1790–1610
Combination oscillation	6400–7700	1560–1300
Second high-order oscillation, stretching oscillation	7800–8900	1280–1120

around 3 mm. Transferring this to an amorphous PA6 sample of 4 mm thickness a transmission of around 26% should be measured.

#### 1.4.5

##### Absorption of NIR-Laser Radiation ( $\lambda = 1200 \text{ nm to } 2500 \text{ nm}$ )

Within the wavelength range of 1200–2500 nm a transition from electronic to molecule oscillation excitation occurs for electromagnetic radiation absorption in polymeric materials. While absorption of electromagnetic radiation at natural plastics can be neglected in the spectral range below 1200 nm, the absorption increased from 1200 to 2500 nm, depending on the molecule structure (see Figure 1.38). For wavelengths more than 2500 nm electromagnetic radiation will be effectively absorbed by excitation of molecule oscillations.

Lightweighted bonding partners in a macromolecule like hydrogen atoms can show extended oscillation amplitudes. Asymmetric oscillation types, where light atoms can oscillate around a strong bond, cause a relative intensive change of the dipole momentum and can be excited by absorption of electromagnetic radiation. In particular, C–H, O–H, S–H and N–H groups in the macromolecule chain can be activated [58]. Base oscillation frequencies of these groups are in the MIR spectral range. But first, higher-order oscillations are in the spectral range between 1550 and 2000 nm and additional higher-order oscillations and combination oscillations are in the spectral range between 800 and 1600 nm.

As an example Table 1.14 summarizes several oscillation types of the C–H group with oscillation frequencies in the spectral range between 1200 and 2500 nm [59].

Excitation of higher-order oscillations in the transition range is considerably weaker than excitation of base oscillations within the MIR spectral range. This causes a deeper penetration of the NIR radiation in polymeric material than MIR radiation.

Figure 1.48 shows as an example the absorption spectra of several thermoplastic resins indicating oscillation types of the C–H group.

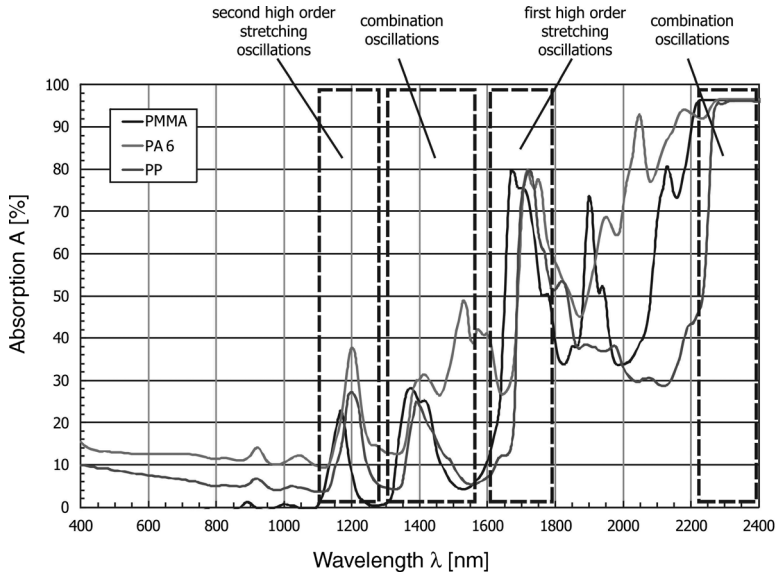


**Figure 1.48** Absorption spectra of natural PMMA, PA6 and PP with indication of C–H group oscillations.

#### 1.4.6

#### Absorption of MIR-Laser Radiation ( $\lambda = 2.5 \mu\text{m}$ to $25 \mu\text{m}$ )

In the spectral range of mid-infrared electromagnetic radiation (MIR spectral range), in which for example is the wavelength of  $\text{CO}_2$  lasers ( $\lambda = 10.6 \mu\text{m}$ ), interaction between electromagnetic radiation and solid polymeric material occurs by excitation of elongation or bending oscillations of individual segments of the macromolecule chains [60]. Table 1.15 summarizes examples of possible chain-segment oscillation types in correlation with their spectroscopic terms.

Generally, oscillation frequencies of oscillators can only be indicated for a frequency range, because the oscillations are influenced by the statistical surrounding of the oscillators within the macromolecular chain. Influencing effects are for example [61]:

- mass of bonding partners neighbor atoms,
- bonding force,
- permanent dipoles in the near surrounding,
- conformation of the molecule chain.

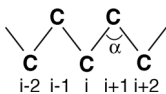


**Figure 1.49** Conformation angle of frame atoms in zigzag conformation.

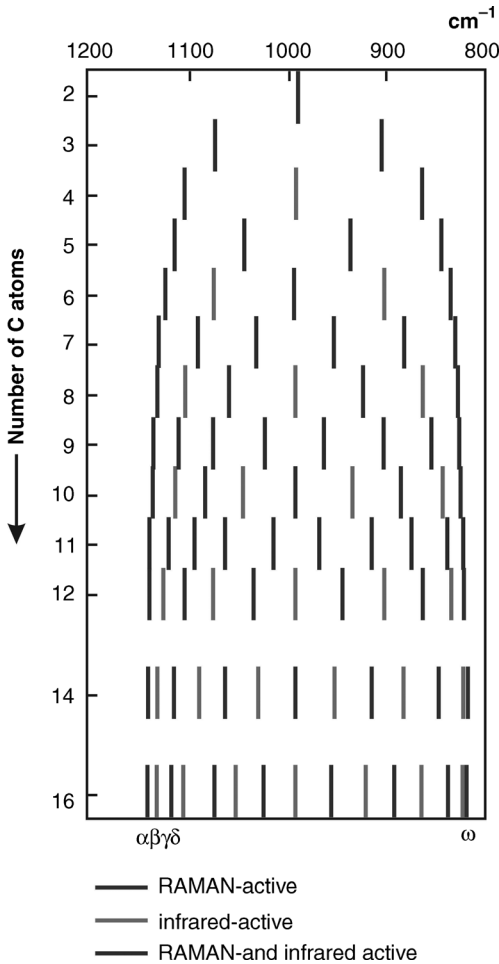


**Figure 1.50** Frequencies of frame oscillations by stretched N-paraffin molecules disregarding the valence angle forces [61].

Out of the entire number of base oscillations only such oscillations can be excited by absorption of IR radiation for which the dipole momentum  $m$  will be changed during an oscillation period [36]. The following considerations will deal only with such IR-active oscillation types, for which the excitation frequency is in the range of the CO<sub>2</sub> laser frequency ( $\nu = 943 \text{ cm}^{-1}$ ,  $\lambda = 10.6 \mu\text{m}$ ).

For absorption of CO<sub>2</sub>-laser radiation, frame oscillations of the molecule chains, group oscillations of side-chain molecules or end-chain molecule oscillations should be considered [61].

The frequency of frame oscillations, for example, for C–C single bonds, is dependent on the number of C atoms within the molecule chain and from the conformation of the molecule chain (see. Figures 1.3 and 1.49 for zigzag conformation):

**Table 1.15** Oscillation types of atoms and atom groups within a molecule chain and their spectroscopic terms [61].

Oscillation type	Term	Geometry
Valence or elongation oscillation	$\nu$	
Deformation or bending oscillation in the bonding plane	$\delta$	
Deformation or bending oscillation vertical to the bonding plane	$\gamma$	
Rocking, tilting or swinging oscillation of a side group	$\varrho$	
Torsion oscillation	$\tau$	

$$\nu = \nu_0 \cdot \sqrt{1 \pm \cos(\alpha) \cdot \cos\left(\frac{\pi \cdot i}{N}\right)} \quad (1.36)$$

$\nu_0$ : base oscillation frequency

$\alpha$ : conformation angle of frame atoms

$i$ : 1, 2, ...,  $N-1$

$N$ : number of C atoms within the chain.

For a molecule chain with  $N$  atoms, which are fixed to their base positions by elastic bonding forces, there result  $3N$  from each other independent base oscillations given by three spatial free oscillation degrees per atom. Translation and rotation oscillations of the entire molecule chain have to be subtracted because these oscillations cause no change of atom distances within the chain and thereby no change of the dipole momentum, generating no contribution to the absorption of electromagnetic radiation. Caused by the symmetrical quality of linear molecule chains the number of possible oscillation frequencies results in  $3N-5$ , while for molecule conformations like zigzag type, helix type or statistical knotted macromolecules (see Figure 1.3) the possible oscillation frequencies results in  $3N-6$  [61].

The oscillation frequency of two C atoms in a molecule chain is at  $\nu = 980 \text{ cm}^{-1}$  ( $\lambda = 10.20 \text{ }\mu\text{m}$ ). With increasing number  $N$  of C atoms the oscillation frequency will be expanded according to Equation 1.36. For a zigzag conformation of the molecule chain with  $N \rightarrow \infty$ , the frequency range will become  $890 \text{ cm}^{-1} < \nu < 1180 \text{ cm}^{-1}$  ( $\lambda = 11.24\text{--}8.47 \text{ }\mu\text{m}$ ) [61] and  $\text{CO}_2$ -laser radiation can be absorbed.

An often occurring end group of molecule chains or their side chains is for example, the methylene group  $\text{CH}_3$  [6]. The oscillation frequency of the methylene group is

**Table 1.16** Frame and group oscillations of polymer chains in the range of the CO<sub>2</sub>-laser wavelength (from [61]). Oscillation frequencies are given as wave numbers (cm<sup>-1</sup>).

Oscillator	Oscillation type	Wave number range cm <sup>-1</sup>
C–C-frame oscillation	Valence oscillation (ν)	890–1150
Methylene group -CH <sub>2</sub>	Deformation oscillation, rocking (ρ)	700–1000
Olefine group X–CH=CH <sub>2</sub> X–CH–CH–X	Deformation oscillation, wagging (g)	905–910 985–995 965–980
Methyl groups –CH <sub>3</sub>	Deformation oscillation, rocking (ρ)	800–1200
Carbonyl group –C–O–H	Deformation oscillation, bonding (δ) wagging (γ)	900–1500 600–1000

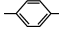
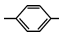
mainly dominated by the angular force constant of the X–C–H bonding angle. The angular force constant itself depends on the influence of the atom X; properties influenced by this are for example, the electron negativity or the atom mass.

Frame oscillations of C atoms within the molecule chain as well as group oscillations of side-chain molecules like methyl or methylene groups have to be considered for absorption of CO<sub>2</sub>-laser radiation [61]. Table 1.16 summarizes possible oscillation types and their frequency range in wave number units.

Additionally Table 1.17 shows for the thermoplastics PC, PA6 and PPS examples of molecule chain components, which can be stimulated to oscillation by absorption of CO<sub>2</sub>-laser radiation.

Oscillation excitation by absorption of electromagnetic radiation is generally depending on the state of the material [61]. For a solid state, like crystalline areas, the macromolecules are mostly present in a zigzag or helical conformation.

**Table 1.17** Thermoplastic polymers and potential structure components that can stimulated to oscillation by absorption of CO<sub>2</sub>-laser radiation.

Polymer	Structure formula	Oscillation type
PA 6	$\left[ \begin{array}{ccccccc} \text{H} & \text{H} & \text{H} & \text{H} & \text{H} & \text{H} & \text{O} \\   &   &   &   &   &   &    \\ -\text{C}- & \text{C}- & \text{C}- & \text{C}- & \text{C}- & \text{N}- & \text{C}- \\   &   &   &   &   & & \\ \text{H} & \text{H} & \text{H} & \text{H} & \text{H} & & \end{array} \right]_n$	–C–C– Frame oscillation
PC	$\left[ \begin{array}{c} \text{O} & \text{CH}_2 \\    &   \\ -\text{O}-\text{C}-\text{O}-\text{C}_6\text{H}_4-\text{C}-\text{C}_6\text{H}_4- \\   &   \\ \text{CH}_2 & \end{array} \right]_n$	–CH <sub>2</sub> Deformation oscillation  Circle deformation oscillation
PPS	$\left[ \text{S}-\text{C}_6\text{H}_4 \right]_n$	 Circle deformation oscillation



Between the molecule chains, forces like hydrogen bridges or dipole bonds exist that can be increased within crystalline areas caused by near-order effects between the molecule chains. By such intermolecular forces, oscillations of atoms or atom groups will be influenced; they can be hindered or the oscillation frequency can be shifted in a way that monochromatic radiation cannot stimulate oscillations [62].

Changing from the solid state into the molten state of thermoplastics the intermolecular forces will be decreased or completely broken up. Molecule oscillations will no longer be hindered and previously inactive oscillations will be activated. Abolition of the geometrical translation symmetry of the molecule chains can additionally activate previously inactive oscillations. The entire absorption of the electromagnetic radiation can be increased by this.

#### 1.4.7

#### **Adaptation of NIR-Radiation Absorption by Additives**

The previous considerations result in the fact that natural thermoplastic polymers have only low absorption within the NIR spectral range from 800 to 1200 nm (see Figure 1.46). Additives for coloration of plastic resins in the visible as well as filler materials and additives for reinforcement of plastics usually don't noticeably increase the absorption in the NIR. In particular, filler materials like glass spheres or fiber reinforcements increase the scattering of NIR radiation in the material but not the absorption.

To enable thermoplastic polymers for laser welding with diode, Nd:YAG or fiber lasers specially suited additives have to be mixed with the resin to increase the absorption of NIR radiation. A couple of suitable additive types like carbon black, inorganic pigments, organic dyes or nanoparticles will be discussed in the following with regard to adapting NIR absorption and influencing the visible appearance of the thermoplastic resin.

##### 1.4.7.1 **Carbon Black**

Carbon black pigments are produced by incomplete combustion and/or thermal decomposition of hydrocarbons [63]. Carbon black pigments consist of carbon and are almost spherical in shape [64].

According to DIN 53206 [65] the structural occurrence of carbon black pigments is distinguished between "primarily particles," "aggregates" and "agglomerates:"

- Primarily particles are the smallest individual particles mostly occurring as spheres with diameter between 10 and 60 nm [66].
- Aggregates are built by cohesion bonding of primarily particles.
- Agglomerates are loose-packed primarily particles or aggregates with dimension of 0.3  $\mu\text{m}$  up to several  $\mu\text{m}$ . Agglomerates can be cut up into smaller particle sizes by scattering for example, during extrusion and molding processes.

Usually, carbon black is used in plastic resins as fine dispersed pigments with typical additive weight proportions in the range between 0.01 and 3%.

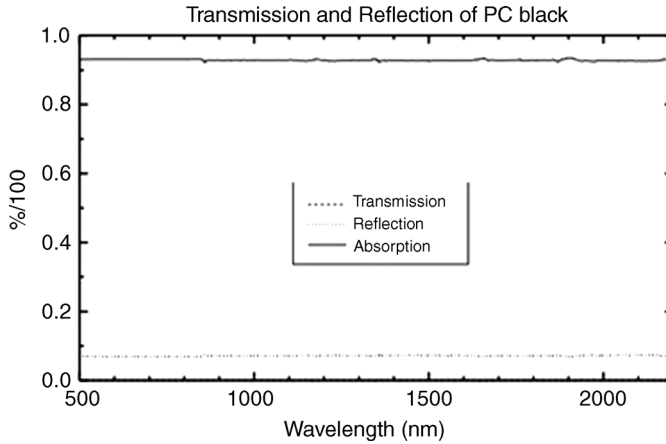


**Figure 1.51** Transmission of carbon black in PC [67].

Carbon black shows a distinctive absorption for electromagnetic radiation over the entire spectral range from UV over VIS up to NIR (Figure 1.51). Caused by the high absorption property of carbon black as additive in plastic materials the optical penetration depth for NIR-laser radiation is typically limited to a range of 10 to some 100  $\mu\text{m}$ , depending on the carbon black concentration. Figure 1.52 shows as an example the optical penetration depth on PP for various carbon black concentrations at the wavelength 940 nm [68].

Because of its economical cost, carbon black is a common used additive to adapt plastic resins for laser welding in various applications like automotive components.

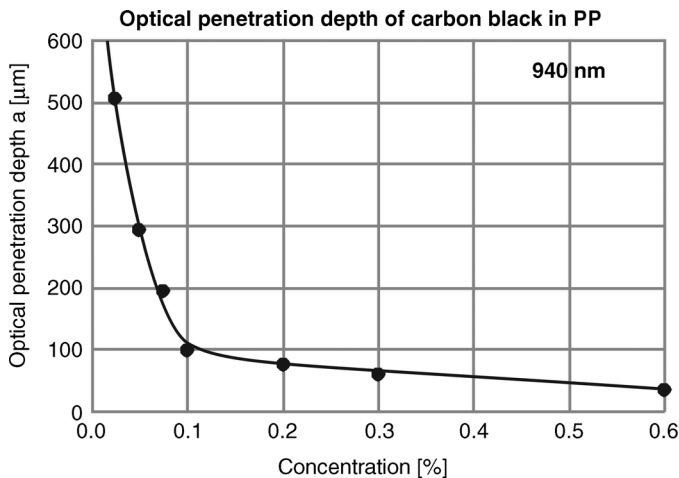


**Figure 1.52** Optical penetration depth on PP with varying carbon black concentration at 940 nm from [68].

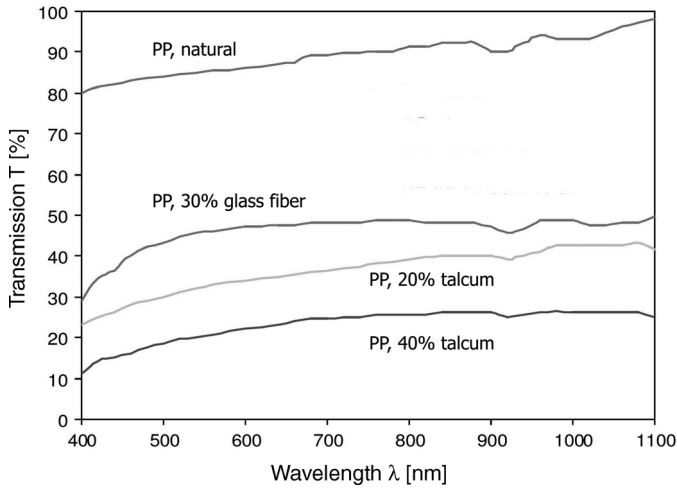


**Figure 1.53** Transmission on PP with varying talcum and titanium dioxide concentration [70].

The disadvantage of carbon black is the black coloration of plastics in the visible for applications like medical devices or other goods where transparency or light coloration are required. Additionally, carbon black influences the electric conductivity of plastics, which can be a disadvantage for use at electric or electronic components.

#### 1.4.7.2 Inorganic Pigments

Inorganic pigments are used as filler materials (e.g., chalk or talcum), functional additives like flame retardants or for visible coloration of plastics. Typical inorganic pigments for coloration are for example, titanium dioxide, iron oxide or other metal oxides [69]. In principle, inorganic pigments are thermally and chemically stable and can be used as additive for a wide range of thermoplastics. Due to their particle size in the range from several  $\mu\text{m}$  to nm inorganic pigments are dispersed in the polymer matrix as individual particles. Inorganic pigments are fixed in position by the polymer matrix and usually migration of the pigments can be neglected.

Typical inorganic pigments don't have a noticeable influence on the absorption of NIR radiation but do increase NIR radiation scattering in the material. Figure 1.53 shows the transmission of PP with various concentrations of talcum in comparison with natural PP and with 30% reinforcement by glass fibers [70]. Increasing pigment concentration results in decreasing transmission caused by internal scattering of the radiation.

Some special inorganic pigments like Lazerflair<sup>®</sup> pigments, copper phosphates or indium tin oxide (ITO) have noticeable absorption of NIR radiation and can be used for enhancing laser weldability of plastics.

Lazerflair<sup>®</sup> pigments are structured as multilayer platelets with a core of glimmer, double-sided coated by metal oxides like  $\text{TiO}_2$  or  $\text{SnO}_2$  (Figure 1.54), having a platelet diameter of around  $15 \mu\text{m}$  and smaller [71].

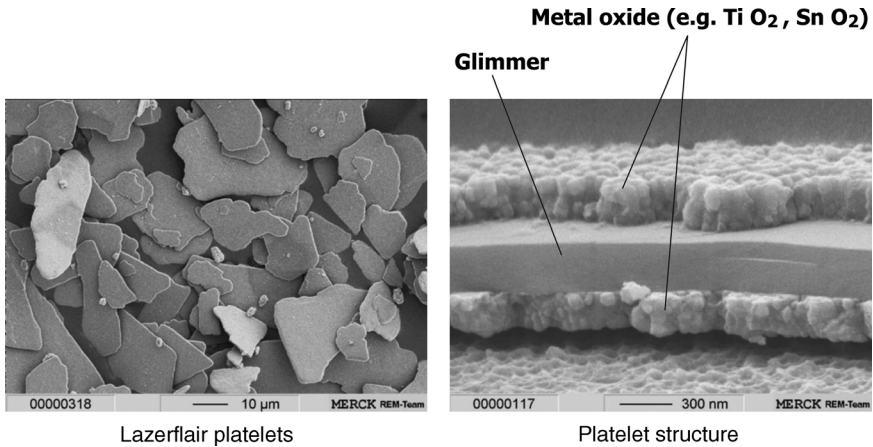


**Figure 1.54** Particle structure of Lazerflair<sup>®</sup> pigments [72].

Typically used Lazerflair<sup>®</sup> concentrations as additive in thermoplastic resins for laser welding are in the range of 0.5–2%, concentrations used for laser marking are below 0.5%. Using low concentration, transmission in the visible is relative high with some influence of internal scattering caused by the pigment size. Increasing concentrations will increase internal scattering, resulting in a noticeable haze on transparent thermoplastic resins.

Lazerflair<sup>®</sup> pigments are broad-band NIR absorbers. For example, Lazerflair<sup>®</sup> 825 has absorption from approximately 900 nm up to 2200 nm. Figure 1.55 shows as an example Lazerflair<sup>®</sup> 825 with concentration of 0.3% in a PP resin with a sample thickness of 1.5 mm.

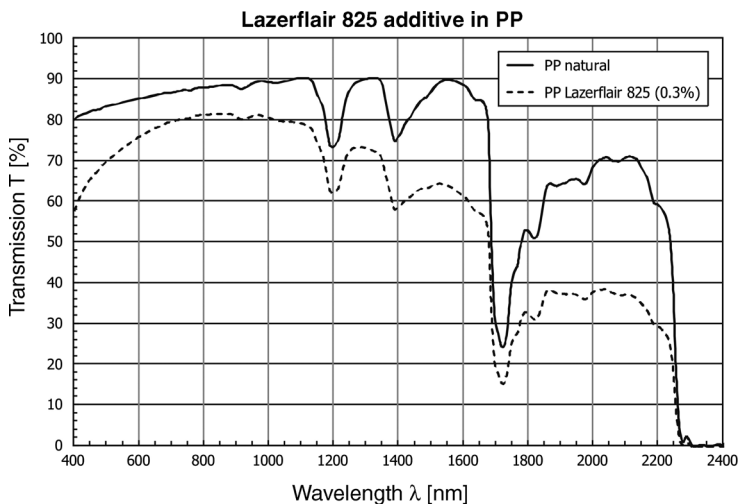


**Figure 1.55** Transmission of Lazerflair<sup>®</sup> 825 in PP, sample thickness 1.5 mm.

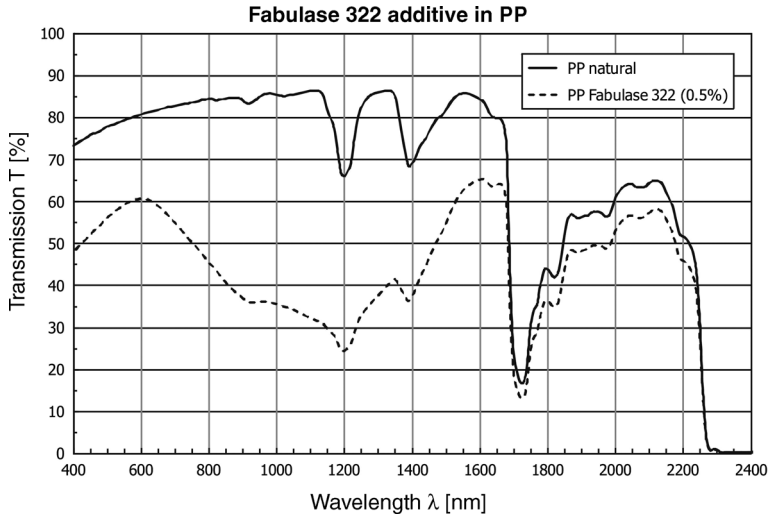


**Figure 1.56** Transmission of FABULASE® 322 in PP, sample thickness 2 mm [73].

Additives based on copper phosphates like FABULASE® 322 have noticeable broad-band absorption for NIR radiation between 900 nm and 1500 nm (Figure 1.56). In the visible they add a slightly green coloration to the resin, depending on the used concentration that is commonly like Lazerflair® in the range of 0.5–2%.

FABULASE® 322 additives are available as powder with pigment sizes smaller than 3 μm and as special micronized powder with particle size smaller than 0.8 μm. Like Lazerflair®, FABULASE® 322 creates a haze in transparent thermoplastics

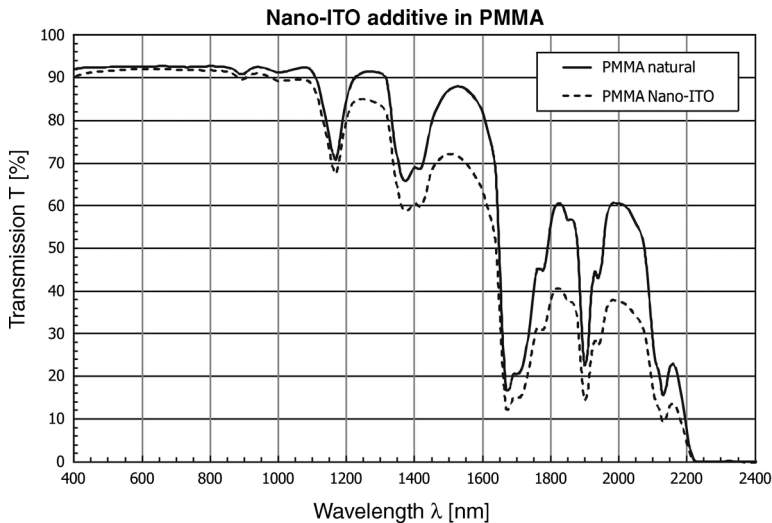


**Figure 1.57** Transmission of nano-ITO particles in PMMA, sample thickness 2 mm.

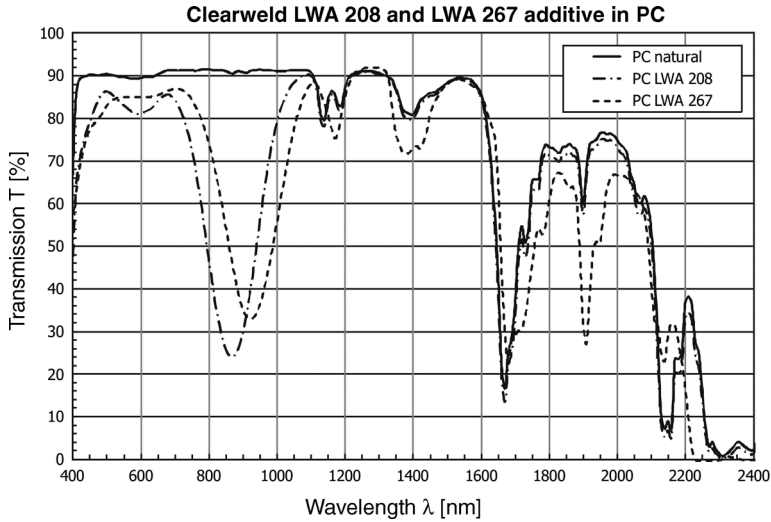


**Figure 1.58** Transmission of Clearweld® A208 and A267 dye in PC, sample thickness 2 mm.

caused by internal scattering of visible radiation. The absorption properties of FABULASE® 322 in the given wavelength area are higher than for Lazerflair® 825.

Indium tin oxide (ITO) is used as nanoscale particles for example, in PMMA and transparent PA resins with low concentrations [74]. As fine dispersed particles with low concentration used for laser marking they add no coloration or haze by internal scattering to the resin because the particle size is much smaller than the wavelength of visible radiation. On increasing concentration for use for laser welding transparent

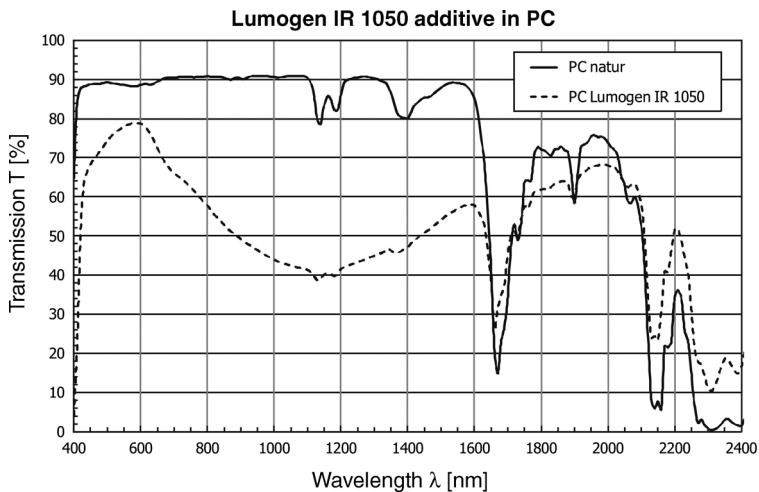


**Figure 1.59** Transmission of Lumogen® IR 1050n nano-pigment in PC, sample thickness 2 mm.

Table 1.18 Absorbing additives and their properties regarding laser welding application.

Additive	Particle size [ $\mu\text{m}$ ]	Absorption range [nm]	Thermal stability	Chemical stability	Visible influence	Can be used in (e.g.,)
Inorganic pigments						
Carbon Black	<0.3	entire spectrum	500	+ + +	Black coloration	All thermoplastics and thermoplastic elastomers
Fabulase 322	<5	900–1600	500	+ + +	Slightly green coloration with influence to hue	PE, PP, PA
Fabulase 322S	<5	900–1600	500	+ + +	Slightly green coloration with some influence to hue	PE, PP, PA
Lazerflair 825	<5	>1000	500	+ + +	Slightly gray coloration with influence to hue	PE, PP, PA
Lazerflair xxx	<5	900–1600	500	+ + +	Slightly green coloration with influence to hue	PE, PP, PA
ITO	<5	>1000	500	+ + +	Transparent colorless	PMMA, PA
Lumogen IR 1050*	<5	900–1500	<800	+ + +	Slightly transparent green coloration	PE, PP, PA
Organic dyes						
Clearweld A267		850–1000	<300	+	Slightly transparent green coloration	PE, PP, PA
Clearweld A225		900–1100	<300	+	Slightly transparent green coloration	PE, PP, PA
Lumogen IR 788		700–810	<350	+ +	Slightly transparent green coloration	PE, PP, PA

thermoplastic resins will get a slightly bluish color with some haze. Nano-ITO additive has a broad-band absorption in the NIR spectral rang from approximately 1000–2000 nm (Figure 1.57).

#### 1.4.7.3 Organic Dyes

Organic dyes like azo, perionon or perylene dyes are used for visible coloration of plastics [69]. Most of organic dyes are restricted in thermally and chemical stability and cannot be used for example, in high-temperature thermoplastics. Organic dyes, built by organic monomers, are dissolved in the polymeric matrix. Due to the state as dye solution in the matrix, internal location changes are possible and migration of organic dyes can occur especially on polyolefin resins and thermoplastic elastomers.

Usually, organic dyes for visible coloration of plastics have no significant absorption in the NIR-radiation region. But there are some special organic dyes (Clearweld® [75–78] and Lumogen® dyes [79–82]) with narrow-band absorption maxima at certain wavelengths in the NIR and less absorption in the visible. Using these dyes as additives with weight percentages between 0.02 and 0.001% will enable thermoplastics for laser welding having neglectable influence of the dye to the visible coloration also for optical transparent thermoplastics like PC or PMMA.

The narrow-band absorption of such organic dyes enables matching the absorption properties of thermoplastic resins to dedicated laser wavelengths like Lumogen® IR 788 and Clearweld® LWA 208 for 808 nm diode lasers or Clearweld® LWA 267 for 940 nm diode lasers. Figure 1.58 shows as an example the transmission spectra of Clearweld® LWA 208 and LWA 267 dyes in PC resin with a sample thickness of 2 mm.

Within the Lumogen IR product family the Lumogen IR 1050 additive is a different type, not built by an organic dye but by a special designed nano-pigment. Figure 1.59 shows the transmission spectra of Lumogen® IR 1050 in PC for a sample thickness of 2 mm.

#### 1.4.7.4 Summarizing Comment

For laser welding of thermoplastics with typically used lasers like diode, Nd:YAG or fiber lasers, the material has to be adapted by suitable additives for absorbing the laser radiation. The several NIR-radiation absorbing additives previously described have different optical, chemical and geometrical properties, which are summarized in Table 1.18.

Depending on the conditions of the prevailing application like laser wavelength used, thermoplastic material, demands on color and transparency and economic aspects, the suitable absorbing additive has to be chosen to adapt the thermoplastic resin to the laser-welding process.

## References

- 1 Frank, A. and Biederbick, K. (1984) *Kunststoffkompendium*, Vogel-Buchverlag, Würzburg.
- 2 Kaufmann, H. (1988) *Grundlagen Der Organischen Chemie*, 8. Auflage, Birkhäuser Verlag, Basel.



- 3 Jarecki, L. (1979) Thermodynamics of deformation of an isolated polymer chain. *Colloid Polym. Sci.*, **257**, 711–719.
- 4 Becker, W. and Braun, D. (1985) *Kunststoff-Handbuch, Bd. 2 Teil 1: Polyvinylchlorid*, 2. Auflage, C. Hanser-Verlag, München.
- 5 Arndt, K.F., Schröder, E., and Körner, A. (1981) Studien zur Verzweigung von Kettenmolekülen. *Acta Polymerica*, **32** (10), pp. 620–625.
- 6 Batzer, C. (1985) *Polymere Werkstoffe Bd.1, Chemie Und Physik*, G. Thieme Verlag, Stuttgart.
- 7 Henrici-Olivè, G. and Olivè, S. (1979) Molecular interactions and macroscopic properties of polyacrylonitrile and model substances, in *Advances in Polymer Science*, Springer Verlag, Berlin.
- 8 Skovranek, D.J., Painter, P.C., and Coleman, M.M. (1986) hydrogen bonding in polymers, 2. Infrared temperature studies of nylon 11. *Macromolecules*, **19**, 699–705.
- 9 Carlowitz, B. (1995) *Kunststoff-Tabellen*, 4. Auflage, C. Hanser Verlag, München.
- 10 DIN EN ISO 1133:2005-09 (D); Kunststoffe - Bestimmung der Schmelze-Masseflussrate (MFR) und der Schmelze-Volumenflussrate (MVR) von Thermoplasten (ISO 1133:2005); Deutsche Fassung EN ISO 1133:2005; Beuth Verlag GmbH, Berlin.
- 11 Menges, G., Haberstroh, E., Michaeli, W., and Schmachtenberg, E. (2002) *Werkstoffkunde Kunststoffe*, 5. Auflage, C. Hanser-Verlag, München.
- 12 Avramova, N. and Fakirov, S. (1981) Melting behaviour of drawn and undrawn annealed nylon 6. *Acta Polymerica*, **32** (6), pp. 318–322.
- 13 Bhowmick, A.K. and Stephens, H.L. (2000) *Handbook of Elastomers*, 2nd edn, CRC-Press, Boca Raton, US.
- 14 Robeson, L.M. (2007) *Polymer Blends: A Comprehensive Review*, Hanser Verlag.
- 15 Albis Guide Chart, Application and Processing of Selected Thermoplastics, company brochure, Albis Plastic GmbH, Hamburg.
- 16 Hagiopol, C. (2000) *Copolymerization*, Springer Press.
- 17 Holden, G., Kricheldorf, H.R., and Quirk, R.P. (2004) *Thermoplastic Elastomers*, 3rd edn, Hanser Verlag.
- 18 ALLOD (2009) Werkstoff GmbH & Co. KG; GRUNDLAGEN TPE; www.allod.com.
- 19 Batzer, H. (1985) *Polymere Werkstoffe, Bd. 3: Technologie II*, Georg Thieme Verlag, Stuttgart.
- 20 Niederstadt, G. (1988) Konstruieren mit Faserverstärkten Polymeren – Das Heterogene Wärmeausdehnungsverhalten als neues Dimensionierungskriterium für Faserverbund-Werkstoffe. Proceedings Verbundwerk '88, Wiesbaden.
- 21 Wunderlich, B. and Baur, H. (1970) Heat capacities of linear high polymers. *Adv. Polym. Sci.*, **7**, 159–368.
- 22 Bergmann, L. and Schäfer, C. (1981) *Lehrbuch Der Experimentellen Physik, Bd. 3v Teil 1 Aufbau Der Materie*, 2. Auflage, De Gruyter Verlag, Berlin.
- 23 VDMA (1979) *Kenndaten Für Die Verarbeitung Thermoplastischer Kunststoffe, Teil 1: Thermodynamik*, C. Hanser Verlag, München.
- 24 Rein, D.M. et al. (1981) The model of polymer crystallisation under non-isothermal conditions. *Acta. Polymerica.*, **32** (1), pp. 1–5.
- 25 Becker, R. (1985) *Theorie Der Wärme*, 3. Auflage, Springer Verlag, Berlin.
- 26 Debye, P. (1912) Zur Theorie der spezifischen Wärme. *Ann. Physik*, **39**, 789.
- 27 Einstein, A. (1907) Die Plancksche Theorie der Strahlung und die Theorie der spezifischen Wärme. *Ann. Physik*, **22**, 180.
- 28 Debye, P. (1914) *Vorträge Über Die Kinetische Theorie Der Materie und Der Elektrizität*, Wolfskehlvorträge, Teubner Verlag, Berlin, pp. 19–60.
- 29 Eiermann, K. (1964) Modellmässige Deutung der Wärmeleitfähigkeit von Hochpolymeren, teil 1: amorphe hochpolymere. *Kolloid-Zeitschrift & Zeitschrift für Polymere*, **198** (1–2), pp. 5–16.
- 30 Eiermann, K. (1964) Modellmässige deutung der wärmeleitfähigkeit von hochpolymeren, teil 2: verstreckte amorphe hochpolymere. *Kolloid-Zeitschrift Zeitschrift für Polymere*, **199** (2), pp. 125–128.
- 31 Knappe, W. (1971) Wärmeleitung in Polymeren. *Adv. Polym. Sci.*, **7**, 477–535.
- 32 Potente, H. (2004) *Fügen von Kunststoffen*, C. Hanser Verlag, München.

- 33 Herziger, G. and Loosen, P. (1993) *Werkstoffbearbeitung mit Laserstrahlung*, C. Hanser Verlag, München.
- 34 Bergmann, L. and Schäfer, C. (1978) *Lehrbuch Der Experimentalphysik, Bd. III Optik*, 7. Auflage, De Gruyter Verlag, Berlin.
- 35 Engelke, F. (1985) *Aufbau der Moleküle*, B. G. Teubner, Stuttgart.
- 36 Born, M. (1981) *Optik*, 3. Auflage, Springer-Verlag, Berlin, Nachdruck der.
- 37 Bunget, I. and Popescu, M. (1984) *Physics of Solid Dielectrics*, Elsevier, Amsterdam.
- 38 Wooten, F. (1972) *Optical Properties of Solids*, Academic Press, New York.
- 39 VDMA (1979) *Kenndaten für die Verarbeitung Thermoplastischer Kunststoffe, Teil 1: Thermodynamik*, C. Hanser Verlag, München.
- 40 Schreyer, G. (1972) *Konstruieren mit Kunststoffen*, C. Hanser Verlag, München.
- 41 Steinfeld, J.I. (1985) *Molecules and Radiation*, 2. Auflage, MIT Press, Cambridge.
- 42 Ben Shaud, A., Haas, Y., Kompa, K.L., and Levine, R.D. (1981) *Lasers and Chemical Change*, Springer Verlag, Berlin.
- 43 Bergmann, L. and Schäfer, C. (1978) *Lehrbuch der Experimentalphysik, Bd. 333 Optik*, 7. Auflage, De Gruyter Verlag, Berlin.
- 44 Günzler, H. and Böck, H. (1983) *IR-Spektroskopie*, 2. Auflage, Verlag Chemie, Weinheim.
- 45 Wooten, F. (1972) *Optical Properties of Solids*, Academic Press, New York.
- 46 Klein, R. (1988) *Kunststoffbearbeitung Mit Laser*, Technika No. 7.
- 47 Lenz, R.W. and Stein, R.S. (1973) *Structure and Properties of Polymer Films*, Plenum Press, New York.
- 48 Adrio, J. (1969) *Strahlungseigenschaften Pigmentierter Kunststoffe Im Bereich Der Temperaturstrahlung*, Dissertation, RWTH Aachen.
- 49 Kreker, M. (1969) *The Scattering of Light*, Academic Press, New York.
- 50 Brügel, W. (1961) *Physik und Technik der Ultrarotstrahlung*, C. R. Vincentz Verlag, Hannover.
- 51 Becker, G.W. and Braun, D. (1988) *Kunststoff-Handbuch, Band 10 Duroplaste*, C. Hanser Verlag, München.
- 52 Batzer, H. (1985) *Polymere Werkstoffe, Bd. 3, Technologie II*, Georg Thieme Verlag, Stuttgart.
- 53 Kaufmann, H. (1988) *Gundlagen der Organischen Chemie*, 8.Auflage, Birkhäuser Verlag.
- 54 Engelke, F. (1985) *Aufbau der Moleküle*, B.G. Teubner, Stuttgart.
- 55 Günzler, H. and Böck, H. (1983) *IR-Spektroskopie*, 2. Auflage, Verlag Chemie, Weinheim.
- 56 Herzberg, G. (1950) *Molekular Spectra and Molecular Structure Bd. 1: Spectra of Diatomic Molecules*, Van Nostrand Reinhold Co., New York/USA.
- 57 Klein, R. (1990) *Bearbeitung von Polymerwerkstoffen mit Infraroter Laserstrahlung*, Dissertation RWTH Aachen.
- 58 Hesse, M., Meier, H., and Zeeh, B. (2005) *Spektroskopische Methoden in Der Organischen Chemie*, Georg Thieme Verlag, Stuttgart.
- 59 Marquardt, J. (2003) *Nah-Infrarot-Spektroskopie für die schnelle Polymeranalytik und die zerstörungsfreie Evaluierung von Materialeigenschaften*, Dissertation Albert-Ludwigs-Universität Freiburg I. Br.
- 60 Hummel, D. (1974) *Polymerspectroscopie*, Verlag Chemie, Weinheim.
- 61 Stuart, H.A. (1967) *Molekülstruktur*, Springer-Verlag, Berlin.
- 62 Steinfeld, J.I. (1985) *Molecules and Radiation*, 2nd edn, MIT Press, Cambridge.
- 63 Ferch, H. (1995) *Pigmentrusse*, Vincentz Verlag, Hannover.
- 64 Klein, H.M. (2001) *Laser Beam Welding of Plastics in Micro Technology*, Thesis, RWTH Aachen.
- 65 N.N. (1996) *DIN 53206*, Beuth Verlag, Berlin.
- 66 Schulz, J.E. (2002) *Material, Process and Component Investigations at Laser Beam Welding of Polymers*, Thesis, RWTH Aachen.
- 67 Staub, H. (2001) *Experimenteller Vergleich des Kontur- und Simultanfügens von Thermoplasten mittels Hochleistungsdiodenlaserstrahlung hinsichtlich Fügbarkeit und*

- Spaltüberbrückbarkeit,  
Diplomarbeit, Fachhochschule  
Würzburg-Schweinfurt.
- 68 Russek, U.A. (2006) *Prozesstechnische Aspekten des Laserdurchstrahlschweißens von Thermoplasten*, Shaker Verlag, Aachen.
- 69 Etzrodt, G. (2003) *Die Farbenwelt der Kunststoffe*, Verlag Moderne Industrie, Landsberg/Lech.
- 70 Russek, U.A., et al. (2007) *Anwenderhandbuch zum Laserschweißen von Kunststoffen*, BMBF-Förderprojekt "Verfahrensoptimierte Werkstoffpaarungen zum Kunststoffschweißen mit Laserstrahlung" FKZ 03N3116.
- 71 Merck KGaA (2009) *When Light Welds - laser Welding of Plastics*, company product brochure June 2009.
- 72 Rosenberger, S. and Hopfner, M. (2005) *Kunststoffe und Pigmentierungen für das Beschriften und Schweißen MIT Laser*. Proceedings Wolf Technologieseminar, Freudenstadt.
- 73 Klein, R. and Wissemborski, R. (2010) *Welding and marking of plastics with lasers*. *Laser Technik Journal*, Sept. 2010 No. 5, Wiley-VCH Verlag, Weinheim.
- 74 Wolff, W. (2005) *Hochtransparente Kunststoffe Dauerhaft Beschriften; Kunststoffe*, 9/2005, Carl Hanser Verlag, München.
- 75 Hoult, A.P. and Burrell, M. (2002) *The effect of diode laser wavelength on the clearweld welding process*. Proceedings ICALEO.
- 76 Woosman, N.M. and Burrell, M. (2003) *A study of the effect of weld parameters on strengths of clearwelded thermoplastics*. Proceedings ICALEO.
- 77 Woosman, N.M. and Sallavanti, R.A. (2003) *Achievable weld strengths for various thermoplastics using the clearweld process*. Proceedings Antec.
- 78 Klein, R. (2007) *Laserstrahlschweißen transparenter und farbiger Kunststoffe*. *Laser Tech. Journal*, Sept. 2007 No. 4, Wiley-VCH Verlag, Weinheim.
- 79 Boehm, A.J. and Edison, M. (2005) *Laser Transmission Welding Of Plastics In Medical Device Manufacturing – How To Choose The Right Laser Additive*, SPE-TopCon.
- 80 Boehm, A.J. and Edison, M. (2005) *The Quaterrylimides – Highly Efficient Nir Absorbers for Laser Transmission Welding of Plastics*, SPE-TopCon.
- 81 Boehm, A.J. and Glaser, A. (2004) *The quaterrylimides – highly efficient NIR absorbers for plastics*. Proceedings Antec.
- 82 Boehm, A.J. (2006) *NIR radiation management part III – rational design of novel NIR absorbers for plastics*. Proceedings Antec.

